A THESIS SUBMITTED TO
THE GRADUATE SCHOOL OF NATURAL AND APPLIED SCIENCES
OF ÇANKIRI KARATEKİN UNIVERSITY

IMPROVED TORQUE AND SPEED PERFORMANCES FOR DTC CONTROLLED ASYNCHRONOUS MACHINE BY FUZZY SWITCHING ALGORITHM

IN PARTIAL FULFILLMENT OF THE REQUIREMENTS
FOR
THE DEGREE OF MASTER OF SCIENCE
IN
ELECTRICAL AND ELECTRONICS ENGINEERING

BY

WAHIB HILOUAN MOHAMED

ÇANKIRI

2022

IMPROVED TORQUE AND SPEED PERFORMANCES FOR DTC CONTROLLED ASYNCHRONOUS MACHINE BY FUZZY SWITCHING ALGORITHM

By Wahib HILOUAN MOHAMED

July 2022

We certify that we have read this thesis and that in our opinion it is fully adequate, in scope and in quality, as a thesis for the degree of Master of Science

Advisor **:** Asst. Prof. Dr. Göksu GÖREL

Examining Committee Members:

Chairman **:** Assoc. Prof. Dr. Fatih KORKMAZ
Electrical and Electronics Engineering
Çankırı Karatekin University

Member **:** Assoc. Prof. Dr. Hayati MAMUR
Electrical and Electronics Engineering
Manisa Celal Bayar University

Member **:** Asst. Prof. Dr. Göksu GÖREL
Electrical and Electronics Engineering
Çankırı Karatekin University

Approved for the Graduate School of Natural and Applied Sciences

Prof. Dr. İbrahim ÇİFTÇİ
Director of Graduate School

I hereby declare that all information in this document has been obtained and presented in accordance with academic rules and ethical conduct. I also declare that, as required by these rules and conduct, I have fully cited and referenced all material and results that are not original to this work.

Wahib HILOUAN MOHAMED

ABSTRACT

IMPROVED TORQUE AND SPEED PERFORMANCES FOR DTC CONTROLLED ASYNCHRONOUS MACHINE BY FUZZY SWITCHING ALGORITHM

Wahib HILOUAN MOHAMED

Master of Science in Electrical and Electronics Engineering

Advisor: Asst. Prof. Dr. Göksu GÖREL

July 2022

Direct torque control is a vector method of control that is based on stator flux and torque. It was pioneered by Takashi in the mid-1980s. Direct selection of the inverter's output voltage vectors allows control of the asynchronous machine's main parameters, especially the stator flux and electromagnetic torque. These decisions are made in such a way that both quantities remain inside a hysteresis band. Our study is mainly concerned with the minimization of the ripple of the electromagnetic torque and stator flux with the use of the direct torque control method that will be applied to the three-phase induction machine. PID controllers and fuzzy logic will produce the best results in terms of reducing ripple at the related torque and speed control. The results will be shown by using Matlab/Simulink at the end of the article, and a discussion will be made by comparing those two regulator.

2022, 76 pages

Keywords: Asynchronous machine, Direct torque control, Fuzzy logic, PI regulator

ÖZET

BULANIK ANAHTARLAMA ALGORITMASI İLE DTC KONTROLÜ ASENKRON MAKİNE İÇİN İYİLEŞTİRİLMİŞ TORK VE HIZ PERFORMANSLARI

Wahib HİLOUAN MOHAMED
Elektrik ve Elektronik Mühendisliği, Yüksek Lisans
Tez Danışmanı: Dr. Öğr. Üyesi. Göksu GÖREL

Temmuz 2022

Doğrudan tork kontrolü, stator akı ve torka dayalı bir vektör kontrol yöntemidir. 1980'lerin ortalarında Takashi tarafından öncülük edilmiştir. İnvertörün çıkış voltajı vektörlerinin doğrudan seçimi, asenkron makinenin ana parametrelerinin, özellikle stator akısı ve elektromanyetik torkun kontrol edilmesini sağlamaktadir. Bu kararlar, her iki nicelik de bir histerezis bandı içinde kalacak şekilde gerçekleştirilir. Çalışmamız temel olarak, üç fazlı asenkron makineye uygulanan doğrudan tork kontrolü nedeniyle elektromanyetik tork ve stator akısının dalgalanmasının azaltmasıyla ilgilidir. PİD ve bulanık mantık denetleyicileri, torktaki dalgalanma azaltılması açısından ve hız kontrolü istenen sonuçları sunacaklar. Sonuçlar makalenin sonunda Matlab/Simulink kullanılarak gösterilip bu iki denetleyici karşılaştırılarak bir tartışma yapılacaktır.

2022, 76 sayfa

Anahtar Kelimeler: Asenkron motoru, Bulanık mantık, Doğrudan moment kontrolü, PI denetleyici.

PREFACE AND ACKNOWLEDGEMENTS

I send my most sincere thanks to my thesis advisor, Asst. Prof. Dr Göksu GÖREL who has been able to support me during my whole period, not only in terms of supervision of my thesis but also by supporting me morally. Then I would like to thank my family for the financial and moral support during my university courses. In addition, my former professor, Assoc. Prof. Dr. Fatih KORKMAZ, from semester 2 of my first year on a subject entitled "The Simulation of the Machine and its Modelling", which was a real profit for the rest of my university period.

Wahib HILOUAN MOHAMED
Çankırı-2022

CONTENTS

LIST OF SYMBOLS

Ns	Synchronous speed
f	Frequency
s	Slip
p	Number of pole pairs
N	Rotor speed
Θ	The angle between stator axes and rotor axes
$\Phi_{as,bs,cs}$	The three phase stator flux
$\Phi_{ar,br,cr}$	The three phase rotor flux
$\Phi_{ds,qs}$	D-q reference stator flux
$\Phi_{dr,qr}$	D-q reference rotor flux
$\overrightarrow{(\Phi_s)}$	Stator flux vector
$\overrightarrow{(\Phi_{s\alpha})}$	Stator flux alpha vector
$\overrightarrow{(\Phi_{s\beta})}$	Stator flux beta vector
$V_{as,bs,cs}$	Three phase stator voltage
$V_{ar,br,cr}$	Three phase rotor voltage
$\mathrm{V_{ds,qs}}$	D-q reference stator voltage
$V_{dr,qr}$	D-q reference rotor voltage
$\overrightarrow{(V_{s\alpha})}$	Voltage source alpha vector
$\overrightarrow{(V_{s\beta})}$	Voltage source beta vector
$I_{as,bs,cs}$	Three phase stator current
$I_{ar,br,cr}$	Three phase rotor current
$\mathrm{I_{ds,qs}}$	D-q reference stator flux
$\mathrm{I_{dr,qr}}$	D-q reference rotor flux
$\overrightarrow{(I_{s\alpha})}$	Stator current alpha vector
$\overrightarrow{(I_{s\beta})}$	Stator current beta vector
Γ_{em}	Electromagnetic torque
$\overrightarrow{(\Gamma_{em})}$	Electromagnetic torque vector
σ	Coefficient of dispersion
L_m	Mutual inductance
L_s	Stator inductance
L_r	Rotor inductance
ω_r	Rotor pulsation speed
ω_s	Stator pulsation speed
l_r	Rotor inductance
m_{rs}	Mutual inductance between two rotor phases

m_{rs}	Mutual inductance between rotor and stator
l_s	Stator inductance
m_s	Mutual inductance between two stator phases
m_{sr}	Mutual inductance between stator and rotor
R_s	Stator resistance
R_r	Rotor resistance

LIST OF ABBREVIATIONS

AC	Alternative current
ASM	Asynchronous machine
DC	Direct current
DTC	Direct torque control
FLC	Fuzzy logic controller
FOC	Field oriented control
FPI	Fuzzified proportional integral
GA	Genetic algorithm
MFs	Membership functions
PID	Proportional integral derivative
SC	Scalar method
SF	Scaling factor
THD	Total harmonic distortion
VSI	Voltage source inverter

LIST OF FIGURES

LIST OF TABLES

1. INTRODUCTION

The essential purpose of electrical machines is the transformation of energy from one form into another, at least one of these forms being electrical, the other being either electrical or mechanical. The operation is based on the laws of electromagnetism. The interaction of electric currents and magnetic fields is what makes them work.

Many different control systems for induction motors have been developed in recent years, and direct torque control has risen to relevance due to its fast dynamic torque feedback and simple control structures. However, the direct torque control approach still has several disadvantages over other control systems, the most significant of which is excessive torque ripple.(Korkmaz, Topaloğlu and Mamur 2015)

Direct torque control (DTC) is a high-performance AC motor drive control technology that was proposed after the vector oriented control scheme within the last 25 years. It was quickly created due to its simple system layout, as well as its transient and dynamic performance. The voltage vector selection table, two hysteresis comparators, and two estimators, one for stator flux and the other for electromagnetic torque, make up the DTC mechanism. DTC uses a Voltage Source Inverter (VSI), space vector and stator flux orientation, and indirect speed regulation to directly control torque and flux. To improve torque and flux performance, a variety of control approaches can be applied. The DTC with Proportional-Integral-Derivative (PID) controller is used in this article to improve the beginning and dynamic performance of an asynchronous motor AM, resulting in good torque and flux response, optimal speed management, and minimal torque ripple. When compared to traditional DTC, the DTC based on PID controller has better IM performance for starting, operating, and changing loads. To improve the performance characteristics of DTC for 3-phase IMD, a PID controller was employed. The performance of DTC with PID controller is analysed under various load circumstances and compared to the performance of traditional DTC. The system demonstrates that a DTC based on a PID controller outperforms a typical DTC in terms of output performance (Abdullah and Ali 2020).

Direct torque control (DTC) has been used in high dynamic performance Induction Motor (IM) drives to provide fast torque response, which is critical in traction and electric vehicle applications. In the traditional DTC, fast torque response can be obtained by improving the selection of the inverter voltage vectors. It proposes a method for selecting voltage vectors in DTC-controlled IM drives in order to obtain quick torque response while maintaining a consistent switching frequency. The use of the Fuzzy PID (FPID) control approach also improves system speed and torque responses. The proposed controller outperforms the traditional DTC in terms of torque and speed responses in simulations. An optimization technique for DTC IM drives quick torque response is shown. In addition, the FPI controller has been modified to work with a speed control loop. Fast torque and speed responses are possible with the suggested system, as well as the usage of a constant switching frequency. When compared to the traditional DTC approach, the system speed and torque responses are vastly enhanced. Theoretical work on voltage vector optimizations as well as Matlab simulations have been completed, confirming the higher performance. Simulations have shown that the suggested solution increases the DTC IM drive's performance. Furthermore, when compared to the PI controller, the FPI controller improves the speed of torque and seed responses (El-Shimy and Zaid 2016).

Based on fuzzy logicthis research proposes a five-level direct torque control (DTC) with 36 induction motor sectors (IM). On the one hand, this intelligence technique was used to fix hysteresis comparators that decrease THD of stator current, torque ripple, and stator flux ripple, while on the other hand, the classic integral proportional (PI) to improve the system's response time period, optimize the closed loop control's performance, and adjust the regulator's parameters to changes in the reference level. The simulation findings back up the correctness of the offered methodologies. A three-phase asynchronous motor operated by a broad-based system is reported in this work. To set up the system, a mathematical model of the converter, sinus pulse width modulation for the three-phase inverter, and a mathematical model of a three-phase asynchronous motor must be used. After constructing such a system, Fuzzy Logic and PID controllers are employed to achieve the desired outcomes, which include a short rotor speed settling time, minimal harmonics, and a short settling time with high phase current. MATLAB Simulink is used to run the mathematical models that have been created. The converter input receives a direct voltage. This voltage is represented by a renewable energy source, such as solar power. The direct voltage is less than the alternating voltage's peak. To drive the induction motor, the alternating voltage is obtained from the inverter's output. The first step is to drive resistive (R) and inductive (L) loads. Second, a low direct voltage is used to drive a three-phase asynchronous motor (ASM). The simulation results are then presented to demonstrate the proposed system's performance and effectiveness. The fuzzy logic-regulating machine's outcomes are compared to the results of the uncontrolled system and the PID system. The fuzzy logic regulating mechanism then produces more desirable outputs. The settling time of a fuzzy controlling machine is faster than the settling time of a PID controlling machine or the settling time of an uncontrolled machine. The time it takes for PID control to settle is faster than the time it takes for uncontrolled settling. The harmonic distortion of a fuzzy logic control system is low. The system has been successfully implemented, according to the observed results. As a result, the investigation yielded good results (Can and Sayan 2016).

Because of its simplicity and ease of implementation, DFIM's traditional DTC control is well-known and widely utilised. Traditional DTC, on the other hand, is generally characterised by high torque and flux ripples, as well as a variable switching frequency. A new combined DTC-GA approach using PI controller improved by genetic algorithm is given to solve the earlier disadvantages of the conventional DTC control. The GA chooses PI values that let traditional DTC perform better. The PI parameters are improved offline, where many values are examined, and then the best PI gains are applied online. Using the Matlab/Simulink environment, the suggested DTC-GA approach for DFIM has been validated. There have been numerous improvements in torque and flux ripple overshoot and response time. Torque and flux ripple have both been reduced by more than 64.44 percent and 50%, respectively. Overshoot in terms of speed and torque has been reduced by nearly 90% and 86 percent, respectively. Direct torque control (DTC) has been used in high dynamic performance Induction Motor (IM) drives to provide fast torque response, which is critical in traction and electric vehicle applications. In the traditional DTC, fast torque response can be obtained by improving the selection of the inverter voltage vectors. The control approach is based on a PI controller that has been modified using a genetic algorithm, and the value optimization of PI parameters is explored in detail. In terms of faster converging speed, high accuracy, and ripple reduction, simulation results showed various improvements in the dynamic response as well as steady-state performance. In comparison to the typical DTC controller, the suggested DTC-GA is more efficient and more likely to be used in electric drives. All performance indexes show that the suggested algorithm outperforms the traditional DTC. However, it is preferable to test it empirically. As a result, we intend to create an experimental prototype in which the PI parameters will be learned and decided using GA in Online mode (or other techniques) (Zemmit, Messalti and Harag 2018).

In both academic and industry circles, fuzzy logic controllers (FLC) have sparked, a lot of interest in the field of machine drive speed control. This is due to FLC's ability to handle nonlinearity and variability. Scaling factors (SFs), membership functions (MFs), and the rule-base are the three primary components of the FLC system. Different sorts and sizes of fuzzy MFs can be created. The most commonly utilised MF sizes for induction motor (IM) speed control are (3x3), (5x5), and (7x7), which are typically developed depending on distribution symmetrical. Varying the breadth and the MFs design’s peak position, on the other hand, improves performance. To boost the effectiveness of the IM drive, the widths and peak positions of the (3x3), (5x5), and (7x7) MFs are asymmetrically dispersed. Based on these MF sizes, the widths and peak positions are changed towards to the origin (zero), negative and positive sides, resulting in a controller that is less susceptible to slight error fluctuations. When compared to the original MFs, the optimised MFs enhanced settling time (Ts) by 5%, rising time by 0.5 percent, and steady-state performance by 20%, according to simulation and achievement tests.

Because of their simple and study design and low maintenance, induction motors have a wide range of applications, and their control systems are attracting a lot of interest from researchers and industries. Controlling the motor's speed, torque, current, and/or flux is what a motor control system does. A traditional controller, such as a PI controller, is typically used to control speed. However, a fuzzy logic controller (FLC) is employed for more adaptive control since it can manage non-linearity, parameter changes, and speed variations. FLC includes scaling factors, membership functions (MFs), and the rule-base. Performance analyses between original MFs and tuned MFs in case of dynamic and steady-state characteristics. Based on simulation and numerical data, tuned MFs improved the dynamic response by 5%, 3.48 %, and 3.68 % settling time optimization and 80.6%, 78.52%, and 50% overshoot adjustment for 3x3, 5x5, and 7x7 MFs, respectively. Furthermore, for all three MF types, the steady state response with tuned MFs has improved by around 20% torque ripple when compared to the original MFs. (Farah *et al*. 2021).

The using method "Fuzzy Logic Technique" is for predicting and controlling motor speed in an induction motor. The dq axis theory is used to model the induction motor. The main goal of this project is to create a fuzzy logic based controller that uses the scalar control model to control the speed of an induction motor. To get the correct speed response, the voltage and frequency input to the induction motor must be regulated. The performance of the developed Fuzzy Logic Controller is also compared to that of a PI controller. A reference speed has been defined for V/f speed control of the induction motor, and the control architecture contains a rule base of 49 rules.

The foundation of the induction motor is investigated, as well as the properties of the induction motor. In MATLAB, the speed response of an induction motor using a fuzzy logic controller (FLC) was properly tested and compared to the speed response of an induction motor using a PI controller. It has been demonstrated that the fuzzy logic controller outperforms the PI controller because the steady state error (SSE) in the FLC is zero, whereas the SSE in the PI controller is roughly 2%. Even the time response in FLC is shorter than in PI controller, indicating that FLC has a faster dynamic reaction than intended PI controller (Aggarwal, Rai and Kandpal 2015).

Switched reluctance (SR) motors are well suited to a wide range of applications due to their inherent simplicity and inexpensive cost. However, due to the motor's dual structure and very nonuniform torque and magnetization properties, it is impossible to excite it using typical AC motor waveforms or apply established AC motor rotating field theory. Furthermore, unless a torque ripple reduction approach is used, the motor will have a large torque ripple. As a result, compared to other machines, controlling the motor is tough and complex. Previous control methods were divided into two categories: those that used a simplified linear model and those that took into account motor saturation. The simpler linear model techniques have the benefit of simplicity and tractability, but they are incorrect in most practical SR drives, whereas the nonlinear systems have the disadvantage of high complexity and computing expense, making real-time implementation problematic. To resolve these concerns, an evaluation of the SR motor's no uniform torque characteristics suggested a new control mechanism for the motor. The control method is based on the direct torque control concept (DTC). The new method does not need short flux patterns, a modification in the motor winding configuration, or the use of a bipolar current drive, unlike earlier direct torque control schemes for the SR motor drive. As a result, the method can be easily implemented on any standard SR motor drive. Furthermore, by limiting the torque output of the motor within a hysteresis range, the approach solves the challenges associated with torque ripple control in the SR motor (Cheok and Fukuda 2002).

To improve the dynamic response and performance of a doubly fed induction motor (DFIM) powered by two voltage source inverters, a new direct torque control (DTC) method is proposed and implemented. Because of its great performance, resilience, and ease of implementation, the DFIM's traditional DTC scheme is extensively utilised. The electromagnetic torque and flux regulated by classical DTC, on the other hand, exhibit large ripples. The combined DTC-backstepping control using a backstepping controller is developed and validated to overcome these drawbacks and to ensure fast response and full reference tracking with the desired dynamic behaviour and low ripple level; this method is focused on the Lyapunov theory to help make sure a powerful control, less sensitivity from machine parameter variation, and no overshoot, unlike traditional PI controllers. Simulation testing using Matlab/Simulink and experimental implementation using the dSPACE DS1104 board will be used to explore the suggested DTC system. Simulation and experimentation results reveal that the suggested control is successful for the DFIM working at varied speeds in terms of rapidity, robustness, and stability (El ouanjli *et al*. 2019).

The application of these machines requires speed control or monitoring to avoid explosion or ignition of the electrical machines. Consequently, power electronics takes on the role of managing these problems. With the advancement of power electronics, the concept of multiphase in motors was introduced, and the first record of multiphase motor controls in the literature is presented in 1969 as an inverter-fed induction motor with five voltage phases (Sarıgül 2021). The electrical machine performs both directions of energy conversion between electrical and mechanical power. It is crucial to keep this energy under control. We control the amount of electric power utilized by motors and the amount of electric power generated by generators. Other factors such as speed, voltages, currents, flux, and torque can be added to the control of electrical devices. Moreover, we will concentrate on a control approach known as direct torque control in this thesis, which will be described in more depth in the next sections (Ghani, Tahour and Colak 2018). Since this requires asynchronous machines to operate under different conditions, various control methods are used. Those methods are discussed in the next part for more details.

The main objective of this thesis is not only to be able to reduce the stator flux and torque ripple by using controllers such as PID and fuzzy logic but also speed control in order to provide a good performance to the asynchronous machine.

This thesis will be divided into 4 major parts. Initially an introduction will be presented and then a literature review will be discussed. In the third part, material and method will be realized and finally the results, which was achieved using matlab simulink, will be presented.

2. LITERATURE REVIEW

2.1 Different Types of Methods For Controlling The Ac Motors

2.1.1 Scalar method

Induction motors have traditionally been employed in applications that require a consistent speed. Their classic speed control methods were neither exceedingly expensive nor terribly inefficient. The goal of induction motor speed control is to obtain the maximum torque and effectiveness. Induction motor drive control has become a hot topic among engineers in recent years. Because of its greater dynamic reaction, several studies have been conducted in the field of vector control systems. The main distinction between scalar and vector control is scalar control's basic structure. Although this control is simple to construct, the inherent coupling of the induction machine variables results in a slow dynamic response, which is a reasonable trade-off in applications such as fans or pumps. Moreover, in given the fact that a mathematical model is preferable for structured control scheme using standard methods, the difficulty of trying to identify accurate parameters for complex nonlinear and time-varying behaviour of real plants may make fine-tuning the model time-consuming in some cases, even when empirical methods are being used. Even if empirical approaches are utilized, the difficulties of defining specific parameters for a complicated nonlinear and time-varying behaviour of real plants may make fine-tuning exceedingly time-consuming in some circumstances. Fuzzy-based control techniques' control performance is less affected by system parameter fluctuations and can cope with nonlinearity. These qualities make system design easier by eliminating the requirement for a precise mathematical model of the plant.

The torque created is load dependent, as it is not directly regulated, which is a disadvantage of scalar control. The transient feedback of this kind of control is also slow due to the inverter's predetermined switching patterns.

However, regardless of whether the over current control loop is implemented, if the rotor motion is continuously blocked, the motor will heat up. The problem of the blocked rotor and load-dependent speed can be solved by adding a speed sensor. This, however, will increase the system's cost, size, and complexity.

The Fuzzy-PI controller has a faster rising time and quicker settling time. More work may be done in this area to speed up the settling time. For includes the practice, the optimal type of inverter can be chosen. This is why neural-based induction motor speed regulation is required.

Scalar technique focuses on the motor's steady-state model. The control is based exclusively on the magnitude variation of the control variables and ignores the machine's coupling effect. For example, a motor's voltage can be adjusted to regulate flux, while its frequency or slip can be adjusted to regulate torque. Flux and torque, on the other hand, are functions of frequency and voltage, respectively. The fundamental coupling effect (i.e., both torque and flux are functions of voltage or current and frequency) causes a poor response, and the system is inclined to instability due to a high-order (fifth-order) system effect, making it much more difficult to implement. As a result, the dynamic performance of the scalar control technique is weak (Yu, Zhang and Qian 2011).

In addition, The SC technique works by keeping the voltage / frequency (V / f) rate constant. The idea is to keep the motor torque constant so that it may be operated at different speeds. When IMs are operated at low speeds, torque production is lowered leading to decreased internal voltage drop, and the motor's dynamic performance is diminished due to disruptive influences such as external load conditions. As a result, the SC approach is utilized in conjunction with other control systems like PID (Proportional-Integral-Derivative). The PID controls, on the other hand, have a low parameter sensitivity. The system can be controlled effectively if the system controller coefficients are properly configured. Any changes in system parameters, on the other hand, have a damaging effect on the controller's performance. The PID control coefficients will need to be readjusted in this scenario (Ötkün 2020). Here the structure of scalar method will be shown below:

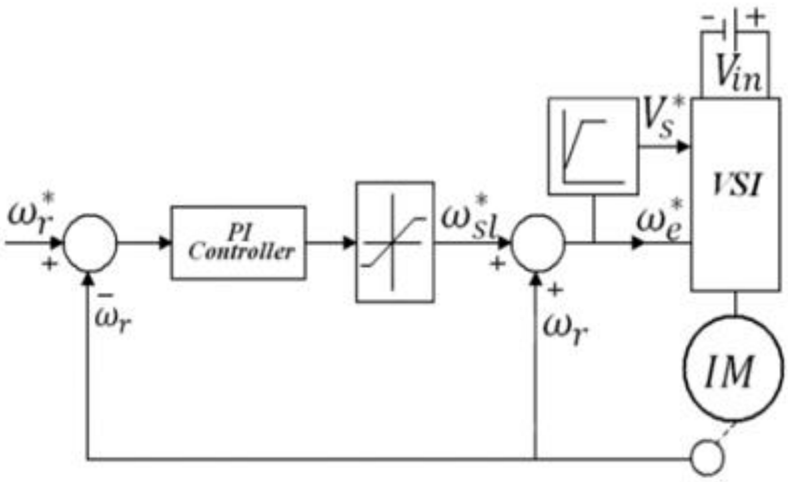

Figure 2.1 Block diagram of controlled scalar of induction machine (Ellabban, Van Mierlo and Lataire 2011).

2.1.2 Vector control

Induction motors can now be used in high-performance applications that previously required only DC drives thanks to vector control techniques. The vector control system allows the induction motor to be controlled in the same manner that individually excitation DC motors are controlled. Torque control induction motors is performed by adjusting the torque current component and flux current component separately, just like in DC motors. Figures 2.2 and 2.3 illustrate the main schemes of indirect and direct vector control systems. The direct vector control approach relies on the stator or air-gap flux signals to generate unit vector signals. The air-gap signals can be directly measured or approximated using stator voltage and current measurements. The stator flux components can be calculated directly from stator values. The rotor speed is not necessary in these systems to collect rotor field angle data. The rotor field angle and hence the unit vectors are derived indirectly in the indirect vector control method by adding the rotor speed and slip frequency. The knowledge of two currents (if the motor is star coupled) and the rotor flux position are essential for the FOC. The FOC relies heavily on knowledge of the rotor flux position. In fact, if this variable is inaccurate, the rotor flux is not aligned with the d-axis, and the current components are estimated incorrectly. Because the rotor speed in an induction machine is not equal to the rotor flux speed (there is a slip speed), a particular method for calculating the rotor flux position (angle) is required. The most simple approach is to use the current model. The torque and flux of induction motors may now be controlled directly and individually thanks to FOC. Every DC machine advantage is obtained by field orientated controlled induction machines: immediate control of the different quantities, allowing accurate transient and steadystate management (Popescu 2000).

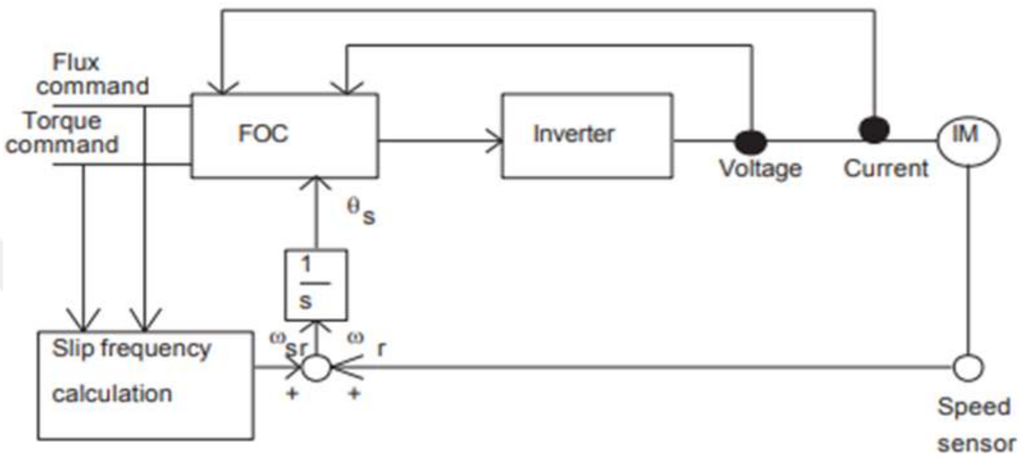

Figure 2.2 Indirect vector control method

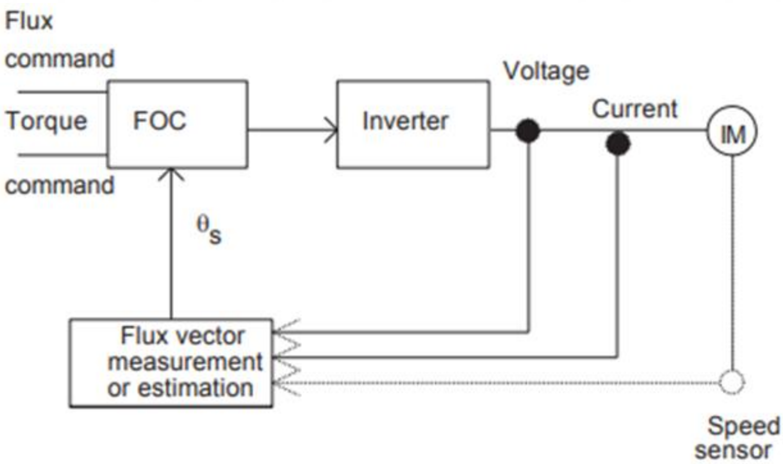

Figure 2.3 Direct vector control method.

2.2 The Different Type of Motors

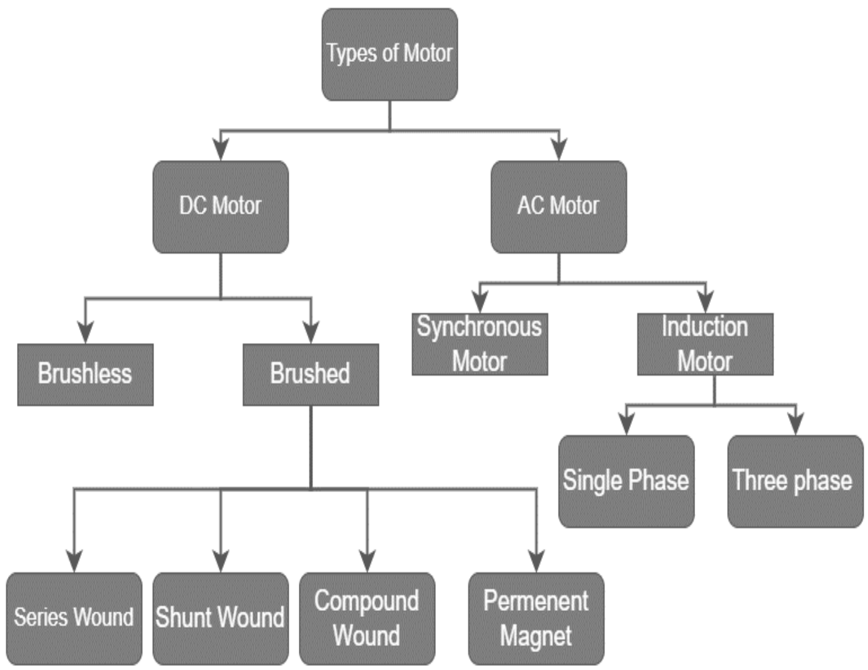

Figure 2.4 Block diagram of the different type of motors.

2.2.1 Ac motors

An AC motor is a motor that uses the electromagnetic induction phenomena to convert alternating current into mechanical power. An alternating current is used to power this motor. AC motors are made up of two major components: the stator and the rotor. The stator is the motor's stationary component, while the rotor is the motor's revolving component. Single-phase or three-phase AC motors are available.

Three-phase AC motors are commonly used in industry to convert bulk power from electrical to mechanical. Single phase AC motors are commonly used for low-power conversion. The single phase AC motor is tiny in size and performs a variety of tasks in the home, office, company, factories, and other settings. Single phase AC motors are used in almost all residential appliances, including refrigerators, fans, washing machines, hair dryers, mixers, and so on (Circuit Globe 2022).

AC motors have great flexibility in terms of features such as speed control and are widely used in industry, compared to DC motors, some of the main advantages are:

- Low start-up power consumption.
- Controlled acceleration
- Adjustable operating speed
- Controlled start-up current
- Adjustable torque limit
- Reduced power line disturbances

Types of AC motors can include:

1) The synchronous motors

When electricity is delivered to a synchronous motor, a revolving field is formed. This field tries to drag the rotor along with it, but it is unable to do so due to rotor inertia. As a result, there is no beginning torque produced. As a result, a self-starting motor is impossible with an inherently synchronous motor. The rotor rotation is synchronized with the supply current's frequency in this type of motor, and the speed remains unchanged under variable loadings, making it perfect for constant speed control equipment. It's also employed in high-precision positioning devices like robot, instrumentations, machinery, and processing control.

2) The asynchronous motors

This motor generates electric current in the rotor and, consequently, torque using electromagnetic induction of the stator winding's magnetic field. Because of its load capacities, it is a widely and importantly used type of alternating current motor in industry, with single-phase induction motors utilised primarily for small loads, such as in household appliances, and three-phase induction motors are employed more in industrial applications like compressors, pumps, conveyor systems, and lifting equipment.

2.2.2 Dc motors

DC motors are the only type of motor to be hugely used and the initial costs of the systems (motor and drive) tend to be lower than AC systems for low power devices, but with higher power devices, the overall maintenance costs increase and should be taken into account. The speed of DC motors can be controlled by varying the supply voltage and they are available in a wide range of voltages. However, the most commonly used voltages are 12 and 24 V, some of the advantages of which are:

- Easy to be installed.
- Wide range of speed control.
- Fast starting, stopping, reversing and accelerating.
- High start-up torque.
- Linear torque-speed curve.

The two most common types are :

1) Brushed motors

They are the most common type of motor and are generally used for low budget applications where the control system is relatively simple, such as consumer applications, and for basic industrial equipment.

This type of motor can be divided as follows:

Series wound: The stator and rotor windings are wired in series. The supply voltage is varied to adjust the speed. This type of motor, on the other hand, offers poor speed control and slows down as the torque applied to it increases. Automobiles, hoists, lifts, and cranes all employ these motors because they require a lot of beginning torque.

Shunt wound: When the motor current is raised, the stator winding is placed in parallel with the rotor winding. This sort of motor may produce larger torque without reducing speed. It is appropriate for applications such as lathes, hoovers, conveyors, and grinders since it has a low starting torque and a steady speed.

Compound wound: This type of motor combines the series excitation structure with the shunt winding structure. The shunt winding's polarity is introduced to the series fields in this way. This motor seems to have a huge beginning torque and can run at a variety of speeds. Compressor, liftings, variable head centrifugal pumpings, rotational pressing, circular saws, shearing machines, and baggage carousels are among the machines that employ it.

Permanent magnet: A permanent magnet, instead of an electromagnet, is employed in applications such as robotic and servo system where accurate estimation and lower torque are required.

2) Brushless

BLDC motors have been increasingly common in industrial and everyday applications, servo systems, and electric cars in recent years. The following are the primary reasons for the growing popularity of BLDC motors, or, in other words, the main benefits of BLDC motors (Korkmaz, 2016)

- High productivity.
- Dense power sources.
- Starting torque is high.
- Variable speeds.
- Characteristics of linear torque and speed.
- Low-maintenance and adaptable to any situation.

Brushless motors eliminate some of the drawbacks of traditional brush motors, such as limited life in heavy-duty applications, and their structural design is considerably easier (brushless). The motor controller detects the rotor’s position using Hall effect sensors, and then regulates the speed of the motor by controlling the current in the rotor winding. Long life, little maintenance, and high performance (85-90 percent) are the benefits of this technology, while high prices and more intricate controllers are the drawbacks. These motors are commonly employed in applications that demand reliability and efficiency, such as fans, pumps, and compressors, for positioning and speed control.

Stepper motors belong to the category of brushless motors. They are mainly used in open loop position control, with applications ranging from printers to industrial applications such as high speed placement equipment (DESIGNSPARK 2016).

3. ASYNCHRONOUS MOTOR

The asynchronous motor is the most widely used motor in industry. It is inexpensive and is manufactured in large series (RESEARCHDIVE 2022). It is robust and requires very limited maintenance. It does not cause sparks, unlike a DC motor. This type of motor is used in almost all conventional machine tools (lathes, milling machines, winding saws, conveyor belts, pumps, compressors, drilling machines, etc.). Operating directly on the AC sector, without prior transformation of the electrical energy that feeds it. The industrial motor does not have delicate parts like the commutator of the DC motor (Proccessing 2022). The currents flowing in the stator are the only external source of magnetic field. Its speed varies a little when it is loaded, it is said to slip, but this slip does not usually exceed a few percentage of the no-load speed and is usually negligible. The starting of asynchronous motors is not a problem for small power units: it is direct. However, for high power motors, it is necessary to start at reduced voltage to avoid too high a current demand.

3.1 The Constitution of An Asynchronous Motor and Its Basic Principles

An asynchronous motor is composed of two main elements, a stator, consisting of windings. This stator has p pairs of poles (i.e. p windings per phase) and a rotor, which is the rotating part of the motor, which is either squirrel cage (smooth bars) or wound. Induction phenomena will be created within the rotor. This is the reason why these machines are also called induction machines. The induced currents flowing in the rotor can only exist if there is a difference in pulsation between the stator and the rotor, in other hand between the stator excitation frequency and the rotor speed.

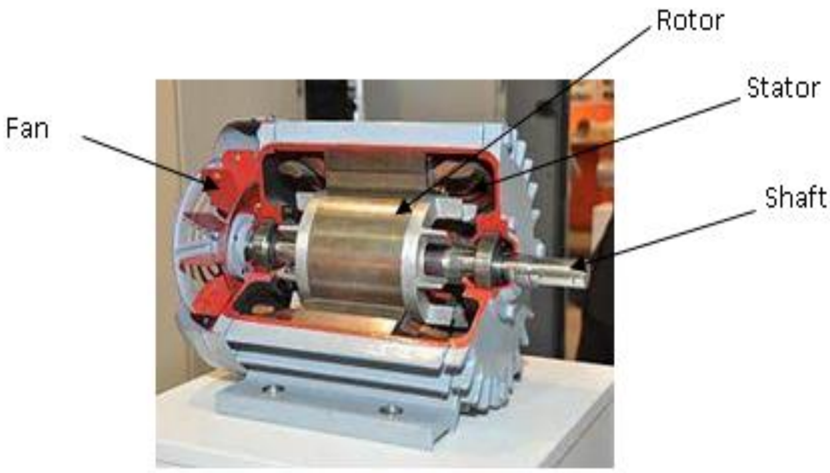

Figure 3.1 The structure of the AC motor.

In any electrical machine, we can always identify a device intended to create the magnetic flux, which is therefore called the "inductor", and a device carrying the conductors, which are the source of electromotive forces due to the effect of induction phenomena, and which is called the "armature". In rotating machines, the inductor and the armature are sometimes fixed (stator) or moving (rotor) according to the construction needs (Mevey 2006).

The stator is the fixed part that constitutes three winding coils, which are positioned at an angle of 120 degrees to each other that create a rotating magnetic field. The rotation frequency is called the synchronism frequency or speed. A relationship is therefore defined in the following formula:

$$N_s = \frac{120f}{p} \tag{3.1}$$

Ns: synchronous speed

p: the number paire of pole.

f: frequence in Hz.

In order for inductive phenomena to occur, we have seen that there must be a difference of speed between the rotor and the magnetic field. This is the slip (s), which can be defined by:

$$s = \frac{N_S - N}{N_S} * 100 \qquad (3.2)$$

With, N rotor speed

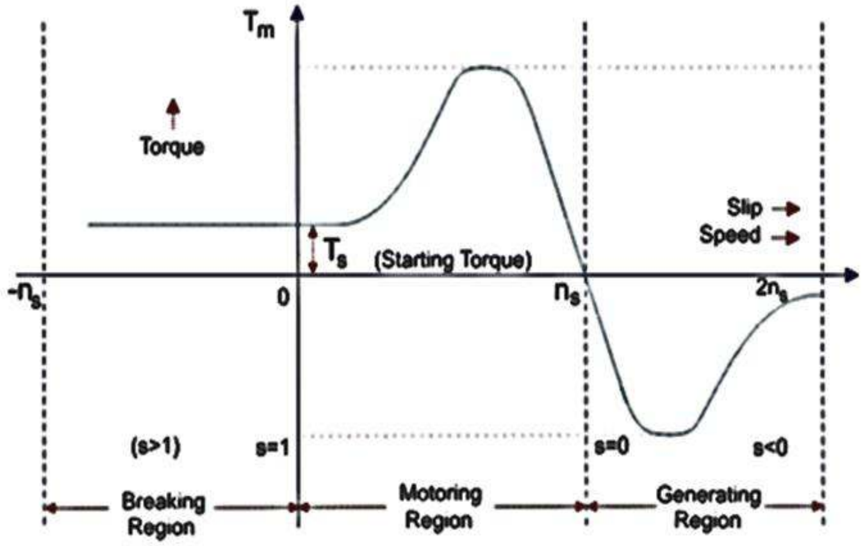

Figure 3.2 Torque-Speed slip curve for three-phase induction motor. (Electrical 4 U 2020).

According to the curve represented above shows us the slip as a function of speed, which aims to define the state of operation of the machine. That is, if the slip is strictly less than zero or negative (s<0) then the machine is in the breaking region. While the machine is said to be in motor operation mode when the slip is between zero and one (0<s<1). In addition, the machine receives a source from outside. Finally when the slip is strictly greater than one the machine is known as a generator (s>1).

3.2 Equivalent Circuit of An Asynchronous Motor

The asynchronous motor must be known for its equivalent circuit to facilitate analysis and be more understandable. This makes the desired calculations (current, moment, power, efficiency) easy to do using the circuit parameters (Bulut 2019)

A phase of an asynchronous motor can be seen as a transformer, whose secondary pulsation secondary would be equal to s*2πf, and that's secondary would be short-circuited.

An equivalent circuit of a single phase belonging to asynchronous machine can be shown below:

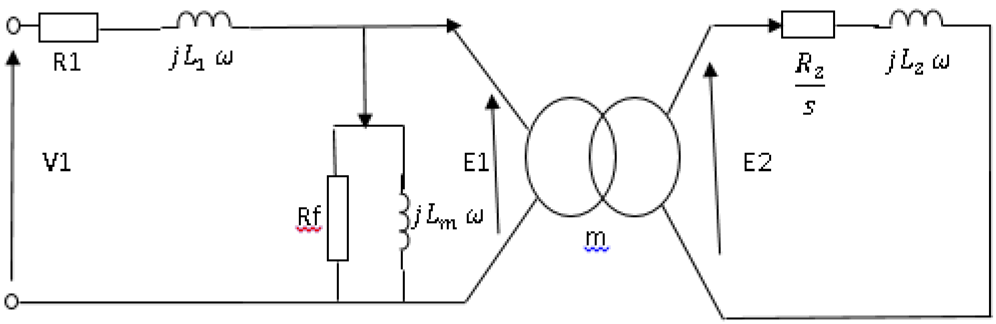

Figure 3.3 Equivalent circuit of a single phase.

For hence,

$R_1 + jL_1\omega$, is the impedance of a stator winding (resistance and leakage inductance).

$\frac{R_2}{s} + jL_2\omega$, is the impedance of a rotor winding (resistance and leakage inductance).

Rf, is the resistance representing the ferromagnetic losses.

$jL_m\omega$, is the resistance representing ferromagnetic losses.

By setting the impedances from the secondary to the primary, we end up with the diagram shown below. Xf represents the leakage reactance of the armature. In this model, the power dissipated in the imaginary resistor R2/s corresponds to the electrical power transmitted to the rotor.

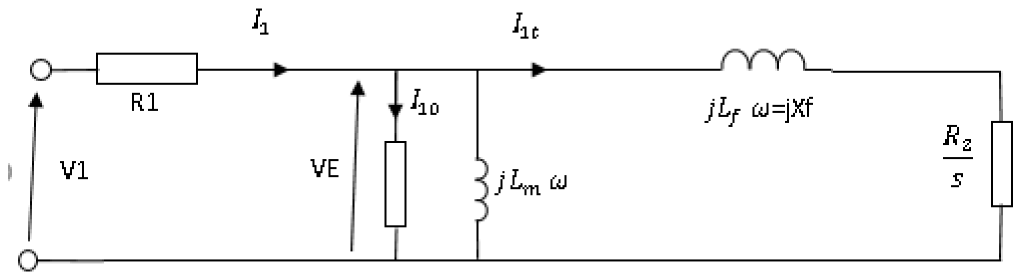

Figure 3.4 A simplified equivalent circuit.

3.3 Mathematical Modelling of The Asynchronous Motor

The modelling of the induction motor is the first essential step for its identification and control. The mathematical model of the machine should have, on the one hand, such a structure in order to comprehensively describe the characteristics of the machine and, on the other hand, it should be practical for the implementation of control and estimation algorithms. When modelling the induction machine, the windings of the three phases of the machine are assumed to be symmetrical (Tallam, Habetler and Harley 2002). Figure 3.5 shows the reference marks and the representation of rotor flux and stator current as space vectors. In Figure 3.5, a, b and c are the axes of the stator windings and α-β are the axes of the fixed reference frame related to the stator, where the α axis was considered to be aligned with the a axis stator winding, d-q is a rotating reference frame related to the magnetic field.

3.3.1 For direct phase (a, b, c)

To begin with, the general expressions of the six winding, stator and rotor, is described as follow (Benzaioua 2014):

$$[V_s] = R_s[I_s] + \frac{d[\Phi_s]}{dt} \tag{3.3}$$

$$[V_s] = R_s[I_s] + \frac{d[\Phi_s]}{dt} \tag{3.4}$$

$$[V_r] = R_r[I_r] + \frac{d[\Phi_r]}{dt} \tag{3.5}$$

Now the expressions for the three-stator windings a, b, c:

$$\begin{cases} V_{as} = R_{as} * I_{as} + d\frac{\Phi_{as}}{dt} \\ V_{bs} = R_{bs} * I_{bs} + d\frac{\Phi_{bs}}{dt} \\ V_{cs} = R_{cs} * I_{cs} + d\frac{\Phi_{cs}}{dt} \end{cases} \tag{3.6}$$

Alternatively, it can be written in matrix form given by this following:

$$\begin{bmatrix} V_{as} \\ V_{bs} \\ V_{cs} \end{bmatrix} = \begin{bmatrix} R_s & 0 & 0 \\ 0 & R_s & 0 \\ 0 & 0 & R_s \end{bmatrix} \begin{bmatrix} I_{as} \\ I_{bs} \\ I_{cs} \end{bmatrix} + \frac{d}{dt} \begin{bmatrix} \Phi_{as} \\ \Phi_{bs} \\ \Phi_{cs} \end{bmatrix} \tag{3.7}$$

With, Rs=Ras=Rbs=Rcs

By applying on the three rotor winding a, b, c, we get an expression shown below:

$$\begin{cases} V_{ar} = R_{ar} * I_{ar} + d\frac{\Phi_{ar}}{dt} \\ V_{br} = R_{br} * I_{br} + d\frac{\Phi_{br}}{dt} \\ V_{cr} = R_{cr} * I_{cr} + d\frac{\Phi_{cr}}{dt} \end{cases} \tag{3.8}$$

It can be written in matrix form given by this following:

$$\begin{bmatrix} V_{ar} \\ V_{br} \\ V_{cr} \end{bmatrix} = \begin{bmatrix} R_r & 0 & 0 \\ 0 & R_r & 0 \\ 0 & 0 & R_r \end{bmatrix} \begin{bmatrix} I_{ar} \\ I_{br} \\ I_{cr} \end{bmatrix} + \frac{d}{dt} \begin{bmatrix} \Phi_{ar} \\ \Phi_{br} \\ \Phi_{cr} \end{bmatrix} \tag{3.9}$$

The magnetic expressions are given in below:

Stator flux expressions:

$$\begin{bmatrix}\Phi_{sa}\\ \Phi_{sb}\\ \Phi_{sc}\end{bmatrix}=\begin{bmatrix}l_s & m_s & m_s\\ m_s & l_s & m_s\\ m_s & m_s & l_s\end{bmatrix}\begin{bmatrix}I_{sa}\\ I_{sb}\\ I_{sc}\end{bmatrix}+\begin{bmatrix}m_{sr}\cos(\theta) & m_{sr}\cos\left(\theta-\frac{4\pi}{3}\right) & m_{sr}\cos\left(\theta-\frac{2\pi}{3}\right)\\ m_{sr}\cos\left(\theta-\frac{2\pi}{3}\right) & m_{sr}\cos(\theta) & m_{sr}\cos\left(\theta-\frac{4\pi}{3}\right)\\ m_{sr}\cos\left(\theta-\frac{2\pi}{3}\right) & m_{sr}\cos\left(\theta-\frac{4\pi}{3}\right) & m_{sr}\cos(\theta)\end{bmatrix}\begin{bmatrix}I_{ra}\\ I_{rb}\\ I_{rc}\end{bmatrix} \quad (3.10)$$

Simplified magnetic expressions of the stator can be defined as:

$$[\Phi_s]=[L_s]\cdot[I_s]+[M_{sr}]\cdot[I_r] \quad (3.11)$$

As,

$$L_s=\begin{bmatrix}l_s & m_s & m_s\\ m_s & l_s & m_s\\ m_s & m_s & l_s\end{bmatrix},\quad I_s=\begin{bmatrix}I_{sa}\\ I_{sb}\\ I_{sc}\end{bmatrix}, I_r=\begin{bmatrix}I_{ra}\\ I_{rb}\\ I_{rc}\end{bmatrix},$$

$$M_{sr}=\begin{bmatrix}m_{sr}\cos(\theta) & m_{sr}\cos\left(\theta-\frac{4\pi}{3}\right) & m_{sr}\cos\left(\theta-\frac{2\pi}{3}\right)\\ m_{sr}\cos\left(\theta-\frac{2\pi}{3}\right) & m_{sr}\cos(\theta) & m_{sr}\cos\left(\theta-\frac{4\pi}{3}\right)\\ m_{sr}\cos\left(\theta-\frac{2\pi}{3}\right) & m_{sr}\cos\left(\theta-\frac{4\pi}{3}\right) & m_{sr}\cos(\theta)\end{bmatrix}$$

l_s: Stator inductance

m_s: Mutual inductance between two stator phases.

m_{sr}: Mutual inductance between stator and rotor.

Rotor flux expressions:

$$\begin{bmatrix}\Phi_{ra}\\ \Phi_{rb}\\ \Phi_{rc}\end{bmatrix} = \begin{bmatrix} l_r & m_r & m_r \\ m_r & l_r & m_r \\ m_r & m_r & l_r \end{bmatrix}\begin{bmatrix}I_{ra}\\ I_{rb}\\ I_{rc}\end{bmatrix} + \begin{bmatrix} m_{rs}\cos(\theta) & m_{rs}\cos\left(\theta-\frac{4\pi}{3}\right) & m_{rs}\cos\left(\theta-\frac{2\pi}{3}\right) \\ m_{rs}\cos\left(\theta-\frac{2\pi}{3}\right) & m_{rs}\cos(\theta) & m_{rs}\cos\left(\theta-\frac{4\pi}{3}\right) \\ m_{rs}\cos\left(\theta-\frac{2\pi}{3}\right) & m_{rs}\cos\left(\theta-\frac{4\pi}{3}\right) & m_{rs}\cos(\theta) \end{bmatrix}\begin{bmatrix}I_{sa}\\ I_{sb}\\ I_{sc}\end{bmatrix} \tag{3.12}$$

$$[\Phi_r] = [L_r]\cdot[I_r] + [M_{rs}]\cdot[I_s] \tag{3.13}$$

As,

$$L_r = \begin{bmatrix} l_r & m_r & m_r \\ m_r & l_r & m_r \\ m_r & m_r & l_r \end{bmatrix},\ I_s = \begin{bmatrix}I_{sa}\\ I_{sb}\\ I_{sc}\end{bmatrix},\ I_r = \begin{bmatrix}I_{ra}\\ I_{rb}\\ I_{rc}\end{bmatrix},$$

$$M_{rs} = \begin{bmatrix} m_{sr}\cos(\theta) & m_{sr}\cos\left(\theta-\frac{4\pi}{3}\right) & m_{sr}\cos\left(\theta-\frac{2\pi}{3}\right) \\ m_{sr}\cos\left(\theta-\frac{2\pi}{3}\right) & m_{sr}\cos(\theta) & m_{sr}\cos\left(\theta-\frac{4\pi}{3}\right) \\ m_{sr}\cos\left(\theta-\frac{2\pi}{3}\right) & m_{sr}\cos\left(\theta-\frac{4\pi}{3}\right) & m_{sr}\cos(\theta) \end{bmatrix}$$

l_r: Rotor inductance

m_r: Mutual inductance between two rotor phases.

m_{sr}: Mutual inductance between rotor and stator.

3.4 Park and Clarke Transformation

In permanent magnet synchronous and asynchronous machines, Clarke and Park transformations are employed in high performance motor designs (vector control). The real (Ids) and imaginary (Iqs) currents can be identified by using Clarke transform. The Park transform can also be used to adjust the spatial relationship between the stator vector current and rotor flow vector by transforming the Ids and Iqs currents from a stationary to a moving reference frame (Microsemi 2013).

The Park transformation refers to a change of variables in the currents, voltages and fluxes involving the angle between the axis of a stator phase and the (d,q) axis system, and is defined by:

$$P(\theta) = \sqrt{\frac{2}{3}}\begin{bmatrix} \cos(\theta) & \cos\left(\theta - \frac{2\pi}{3}\right) & \cos\left(\theta + \frac{2\pi}{3}\right) \\ -\sin(\theta) & -\sin\left(\theta - \frac{2\pi}{3}\right) & -\sin\left(\theta + \frac{2\pi}{3}\right) \end{bmatrix} \quad (3.14)$$

The angle θ in the matrix P(θ) takes the value θ_s for the stator quantities and the value $(\theta_s - \theta_r)$ For the rotor quantities.

The inverse of this matrix gives us

$$P(\theta)^{-1} = \sqrt{\frac{2}{3}}\begin{bmatrix} \cos\theta & -\sin\theta \\ \cos\left(\theta - \frac{2\pi}{3}\right) & -\sin\left(\theta - \frac{2\pi}{3}\right) \\ \cos\left(\theta + \frac{2\pi}{3}\right) & -\sin\left(\theta + \frac{2\pi}{3}\right) \end{bmatrix} \quad (3.15)$$

The Park transformation consists of a three-phase - two-phase Clark or Concordia transformation followed by a rotation. It allows to go from the abc reference frame to the α-β reference frame and then to the d-q reference frame (Khlaeif *et al*. 2011). The α-β frame is always fixed with respect to the a-b-c frame, whereas the d-q frame is mobile. It forms an angle with the fixed frame α-β, which is called the angle of the Park transformation or Park angle.

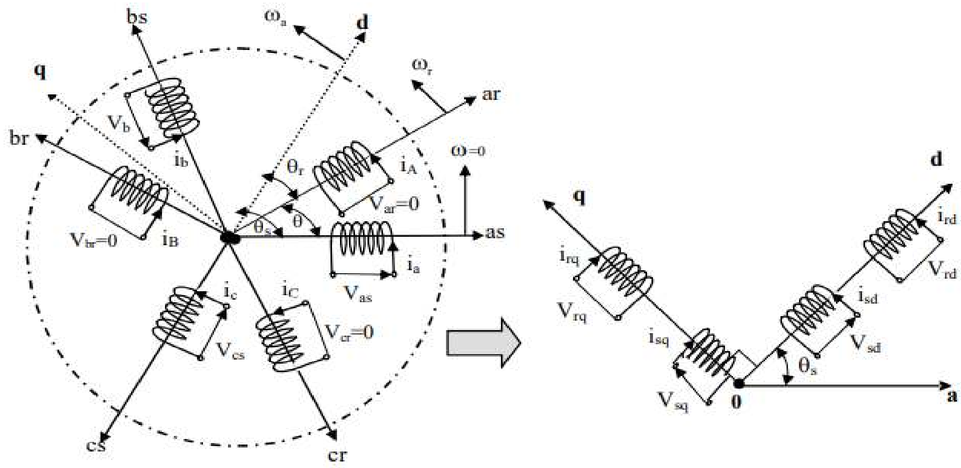

Figure 3.5 From a-b-c reference frame to d-q reference frame equivalent model (Abdesselem 2008).

The Clarke transform's two phases, frame representation is then input into a vector rotation block and turned over an angle to follow the frame d,q tied to the rotor flux (Texas Instruments 1997). The transformation from a fixed frame (α, β) to a rotating frame {d, q) at speed ω, also known as the PARK transformation, is given:

$$\begin{bmatrix} I_{ds} \\ I_{qs} \end{bmatrix} = \begin{bmatrix} cos\theta & sin\theta \\ -sin\theta & cos\theta \end{bmatrix} \begin{bmatrix} I_{s\alpha} \\ I_{s\beta} \end{bmatrix} \tag{3.16}$$

The Park transform applied on the AC motor’s expressions can be described as follows:

$$[P(\theta)][V_{dq}] = [R][I_{dq}][P(\theta)] + \frac{d[[P(\theta)][\Phi_{dq}]]}{dt} \tag{3.17}$$

$$[V_{dq}] = [R][I_{dq}] + [P(\theta)^{-1}]\frac{d[[P(\theta)]]}{dt}[\Phi_{dq}] \tag{3.18}$$

$$[P(\theta)^{-1}]\frac{d[[P(\theta)]]}{dt} = \begin{bmatrix} 0 & -1 & 0 \\ 1 & 0 & 0 \\ 0 & 0 & 0 \end{bmatrix} * \frac{d\theta}{dt} \tag{3.19}$$

As,

$\theta = \theta_s$ For stator value.

θ = ($\theta_s - \theta_r$) For rotor value.

Then when we replace from the expressions cited above then we get the followings expressions described below:

$$V_d = RI_d + \frac{d\Phi_d}{dt} - \frac{d\theta}{dt}\Phi_q \tag{3.20}$$

$$V_q = RI_q + \frac{d\Phi_q}{dt} - \frac{d\theta}{dt}\Phi_d \tag{3.21}$$

Therefore, we make expressions for stator and rotor based on d-q reference frame and we obtain for each of them the following expressions:

For the stator

$$V_{ds} = RI_d + \frac{d\Phi_{ds}}{dt} - \frac{d\theta_s}{dt}\Phi_{qs} \tag{3.22}$$

$$V_{qs} = RI_{qs} + \frac{d\Phi_{qs}}{dt} + \frac{d\theta_s}{dt}\Phi_{ds} \tag{3.23}$$

For the rotor,

$$V_{dr} = 0 = RI_{dr} + \frac{d\Phi_{dr}}{dt} - \frac{d\theta}{dt}\Phi_{qr} \tag{3.24}$$

$$V_{qr} = 0 = RI_{qr} + \frac{d\Phi_{qr}}{dt} + \frac{d\theta}{dt}\Phi_{dr} \tag{3.25}$$

Let us keep applying the Park transformation on the flux expressıons; it can be expressed as follow:

$$\begin{cases} [\Phi_{dqs}] = [P(\theta)][\Phi_s] \\ [\Phi_{dqr}] = [P(\theta)][\Phi_r] \end{cases} \tag{3.26}$$

For the stator flux

$$[\Phi_{dqs}] = [P(\theta)]([l_s][I_s] + [M_{sr}][I_r\ ]) \tag{3.27}$$

For the rotor flux

$$\left[\Phi_{dqr}\right] = [P(\theta)]([l_r\ ][I_r\ ] + [M_{rs}\ ][I_s\ ]) \tag{3.28}$$

The above expressıons after being developed and regrouped gives us the following expressıons:

$$\begin{bmatrix}\Phi_{ds}\\ \Phi_{qs}\\ \Phi_{dr}\\ \Phi_{qr}\end{bmatrix} = \begin{bmatrix} l_s - M_s & 0 & \frac{3}{2}M_{sr} & 0 \\ 0 & l_s - M_s & 0 & \frac{3}{2}M_{sr} \\ \frac{3}{2}M_{sr} & 0 & l_r - M_r & 0 \\ 0 & \frac{3}{2}M_{sr} & 0 & l_r - M_r \end{bmatrix} \begin{bmatrix} I_{ds}\\ I_{qs}\\ I_{dr}\\ I_{qr}\end{bmatrix} \tag{3.29}$$

By putting as,

$L_s = l_s - M_s$, stator inductance

$L_r = l_r - M_r$, rotor inductance

$L_m = \frac{3}{2}M_{sr}$, mutual inductance between the stator and the rotor.

Then, the formula becomes:

$$\begin{bmatrix}\Phi_{ds}\\ \Phi_{qs}\\ \Phi_{dr}\\ \Phi_{qr}\end{bmatrix} = \begin{bmatrix} L_s & 0 & L_m & 0 \\ 0 & L_s & 0 & L_m \\ L_m & 0 & L_r & 0 \\ 0 & L_m & 0 & L_r \end{bmatrix} \begin{bmatrix} I_{ds}\\ I_{qs}\\ I_{dr}\\ I_{qr}\end{bmatrix} \tag{3.30}$$

By replacing the flux formula in the voltage expressions, we get:

$$\begin{bmatrix} V_{ds} \\ V_{qs} \\ V_{dr} \\ V_{qr} \end{bmatrix} = \begin{bmatrix} R_s + L_s \frac{d}{dt} & -L_s \frac{d\theta_s}{dt} & L_m \frac{d}{dt} & -L_m \frac{d\theta}{dt} \\ L_s \frac{d\theta_s}{dt} & R_s + L_s \frac{d}{dt} & L_m \frac{d\theta}{dt} & L_m \frac{d}{dt} \\ L_m \frac{d}{dt} & -L_m \frac{d\theta}{dt} & R_r + L_r \frac{d}{dt} & -L_r \frac{d\theta}{dt} \\ L_m \frac{d\theta}{dt} & L_m \frac{d}{dt} & L_r \frac{d\theta}{dt} & R_r + L_r \frac{d}{dt} \end{bmatrix} \begin{bmatrix} I_{ds} \\ I_{qs} \\ I_{dr} \\ I_{qr} \end{bmatrix} \tag{3.31}$$

The rotor being short-circuited the expressions can be written as:

$$\begin{bmatrix} V_{ds} \\ V_{qs} \\ 0 \\ 0 \end{bmatrix} = \begin{bmatrix} R_s + L_s \frac{d}{dt} & -L_s \omega_s & L_m \frac{d}{dt} & -(\omega_s - \omega_r) L_m \\ L_s \omega_s & R_s + L_s \frac{d}{dt} & (\omega_s - \omega_r) L_m & L_m \frac{d}{dt} \\ L_m \frac{d}{dt} & -(\omega_s - \omega_r) L_m & R_r + L_r \frac{d}{dt} & -(\omega_s - \omega_r) L_r \\ (\omega_s - \omega_r) L_m & L_m \frac{d}{dt} & (\omega_s - \omega_r) L_r & R_r + L_r \frac{d}{dt} \end{bmatrix} \begin{bmatrix} I_{ds} \\ I_{qs} \\ I_{dr} \\ I_{qr} \end{bmatrix} \tag{3.32}$$

With $\omega_s = \frac{d\theta_s}{dt}$ and $\omega_s - \omega_r = \frac{d\theta}{dt}$

The currents can be expressed in term of fluxes as follows:

$$\begin{cases} I_{ds} = \frac{1}{\sigma L_s} \Phi_{ds} - \frac{1-\sigma}{\sigma L_m} \Phi_{dr} \\ I_{qs} = \frac{1}{\sigma L_s} \Phi_{qs} - \frac{1-\sigma}{\sigma L_m} \Phi_{qr} \\ I_{dr} = \frac{1}{\sigma L_s} \Phi_{dr} - \frac{1-\sigma}{\sigma L_m} \Phi_{ds} \\ I_{qr} = \frac{1}{\sigma L_s} \Phi_{qs} - \frac{1-\sigma}{\sigma L_m} \Phi_{qr} \end{cases} \tag{3.33}$$

With, $\sigma = 1 - \frac{L_m^2}{L_s L_r}$:coefficient of dispersion.

From the Equation (3.32), it becomes

$$\begin{cases} \frac{d\Phi_{ds}}{dt} = -R_s I_{ds} + \frac{d\theta_s}{dt} \Phi_{qs} + V_{ds} \\ \frac{d\Phi_{ds}}{dt} = -R_s I_{qs} + \frac{d\theta_s}{dt} \Phi_{ds} + V_{qs} \\ \frac{d\Phi_{dr}}{dt} = -R_r I_{dr} + \frac{d\theta}{dt} \Phi_{qr} \\ \frac{d\Phi_{qr}}{dt} = -R_r I_{qr} + \frac{d\theta}{dt} \Phi_{dr} \end{cases} \tag{3.34}$$

In order to realize this study, a reference should be selected. There are three types of reference; it will be discussed for more details.

a. Reference related to stator (stationary reference)

This frame of reference is chosen when studying variations in the speed of rotation, whether or not associated with variations in the supply frequency.

$$\frac{d\theta_s}{dt} = 0$$

$$\frac{d\theta}{dt} = \frac{d(\theta_s - \theta_r)}{dt} = -\omega_r$$

b. Reference related to rotor.

This frame of reference is interesting in problems where the speed of rotation is considered constant, for example when studying the forces of a short circuit.

$$\frac{d\theta_s}{dt} = \omega_s$$

$$\frac{d\theta}{dt} = \frac{d(\theta_s - \theta_r)}{dt} = -\omega_r = 0$$

c. Reference related to rotating field (magnetic field)

It is very interesting in applications where the supply frequency is constant, which simplifies the calculations considerably. It is also used in static frequency converter power supply problems of asynchronous motors by static frequency converters when we want to study the transfer function of the motor with respect to small disturbances around a given speed (Toufouti, Meziane and Benalla 2006).

$$\frac{d\theta_s}{dt} = \omega_s$$

$$\frac{d\theta}{dt} = \frac{d(\theta_s - \theta_r)}{dt} = -\omega_r$$

We will choose this frame of reference because it is best suited to our study.

The purpose of the asynchronous machine model is to establish the performance and mathematical modeling in steady state that we can expect from a real actuator; in our work, we have chosen a reference frame stationary to the rotating field, in order to be able to orientate the rotor flux. The expresions shown below will be written as follows:

$$X^{\cdot} = AX + BU$$

$$\begin{cases} \frac{di_{ds}}{dt} = \left(-\frac{1}{\sigma T_s} - \frac{(1-\sigma)}{T_r}\right) i_{ds} + \omega_s i_{qs} + \frac{1-\sigma}{\sigma L_m T_r} \Phi_{dr} + \frac{1-\sigma}{\sigma L_m} \omega_r \Phi_{qr} + \frac{1}{\sigma L_s} V_{ds} \\ \frac{di_{qs}}{dt} = -\omega_s i_{ds} + \left(-\frac{1}{\sigma T_s} - \frac{(1-\sigma)}{T_r}\right) i_{qs} - \frac{1-\sigma}{\sigma L_m} \omega_r \Phi_{dr} + \frac{1-\sigma}{\sigma L_m T_r} \Phi_{qr} + \frac{1}{\sigma L_s} V_{qs} \\ \frac{d\Phi_{dr}}{dt} = \frac{L_m}{T_r} i_{ds} - \frac{1}{T_r} \Phi_{dr} + (\omega_s - \omega_r)\Phi_{qr} \\ \frac{d\Phi_{qr}}{dt} = \frac{L_m}{T_r} i_{qs} - (\omega_s - \omega_r)\Phi_{dr} - \frac{1}{T_r} \Phi_{qr} \end{cases} \tag{3.35}$$

With, $T_r = \frac{L_r}{R_r}$ and $T_s = \frac{L_s}{R_s}$

The electromagnetic torque and mechanical pulsation of the rotor can be expressed as:

$$\Gamma_{em} = \frac{3pL_m}{2L_r}\left(I_{qs}\,\Phi_{dr} - I_{ds}\,\Phi_{qr}\right) \tag{3.36}$$

$$\omega_r = \frac{3p^2 L_m}{2JL_r}\left(I_{qs}\Phi_{dr} - I_{ds}\Phi_{qr}\right) \tag{3.37}$$

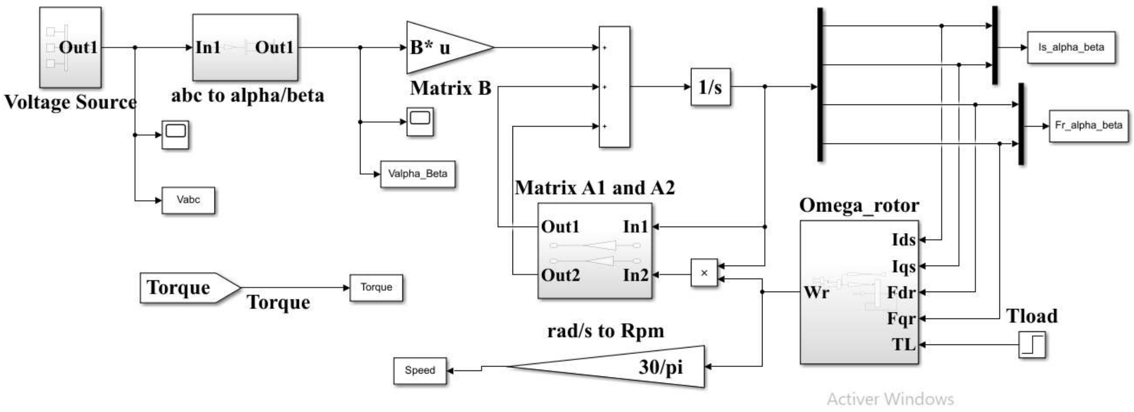

Figure 3.6 Representation of three phase ASM under voltage source on Simulink.

4. MATERIALS AND METHODS

4.1 Direct Torque Control Applied On Asynchronous Motor

4.1.1 Introduction

The Direct Torque Control (DTC) technique was initiated by TAKAHASHI in the mid-1980s. Recently, it is increasingly used in industry in place of other types, in particular Field Oriented Control (FOC) (Rehman and Xu 2011). Several studies have allowed a detailed modelling of this control technique, which exploits the ability to apply torque and flux to AC machines in a decoupled manner, when fed by voltage inverter without the use of a feedback loop for current regulation, achieving performance similar to that of vector controls. The DTC consists of calculating the control quantities of stator flux and electromagnetic torque from stator current measurements without the use of mechanical sensors. The only drawback could be seen in DTC structure is that the starting torque is high.

In the DTC structure, the asynchronous machine controlled by the voltage inverter is a hybrid dynamic system, of which the continuous part is the asynchronous machine and the discrete part is the voltage inverter.

This essential part will be devoted to the description of the DTC control applied on the three-phase asynchronous machine.

4.1.2 Direct torque control's principle

The method of control is to directly regulate the electromagnetic torque and stator flux by directly determining the control sequence applied on the switches of a voltage inverter (Hu *et al*. 2010). This choice is based on the use of hysteresis comparator whose role is to control the state of the system, namely the stator flux amplitude and the electromagnetic torque. It is a question of keeping these two quantities within defined error ranges. It means that the two controller outputs combined with information on the position where the flux vector was positioned in order to determine the switching table required to operate the inverter. This inverter (Two-level inverter) allows for seven distinct positions in the desired sector, corresponding to the eight sequences of the voltage vector at the inverter's output. Direct torque control of a three-phase asynchronous machine can be illustrated in the following scheme:

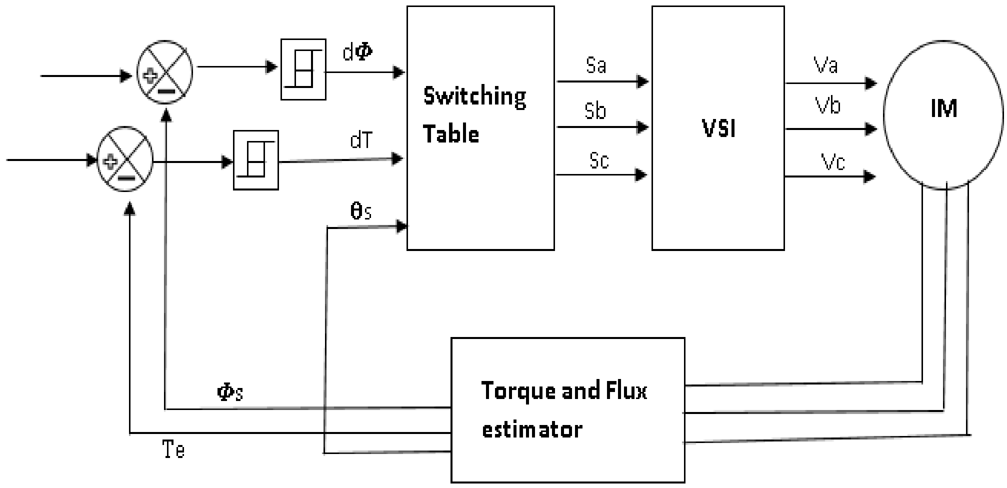

Figure 4.1 The basic scheme of conventional DTC.

4.1.3 The voltage source inverter

The VSI is used to generate the three-phase voltage that drives the motor. The VSI is considered as a perfect source or a power supply that it will be benefit for the rest of this part and it will shown in Figure 4.2, consisting of two generators equal to E/2 connected to a point noted no (neutral point). In practice, several switch technologies are used like IGBT (insulated gate bipolar transistor) or MOS (metal-oxide semiconductor) (Brown *et al*. 2011).

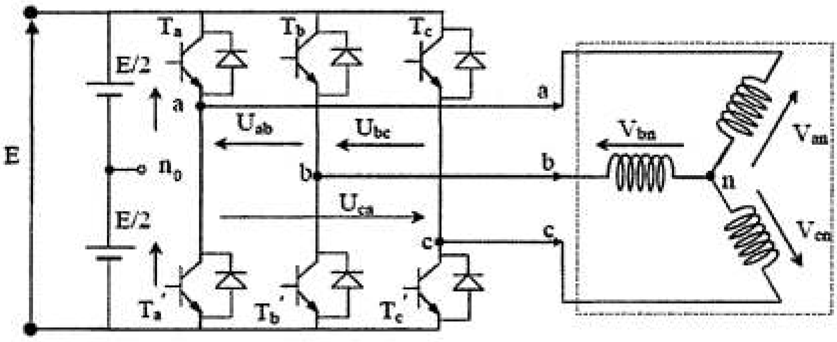

Figure 4.2 The structure of inverter based on Switching states.

The role of the inverter shown in Figure 4.2 is to supply simple AC voltages noted Van, Vbn and Vcn to the motor, from a DC voltage E (supplied by a rectifier or another DC supply). The voltages supplied by the inverter form a three-phase system of variable frequency and amplitude.

The inverter is controlled by the logic inputs Si. We call Ti and T, the transistors (assumed to be ideal switches), we have:

If Si=1, Ti is passing and Ti' is open.

If Si=0, Ti is open and Ti' is passing.

With i=a, b, c.

The combination of the different states of the inverter gives 2^3=8 possible cases for the voltage vector Vs, of which two vectors are zero (V0 and V7) and six are non-zero. Figure 4.3 shows the six non-zero vectors that can be generated by a three-phase two-level inverter.

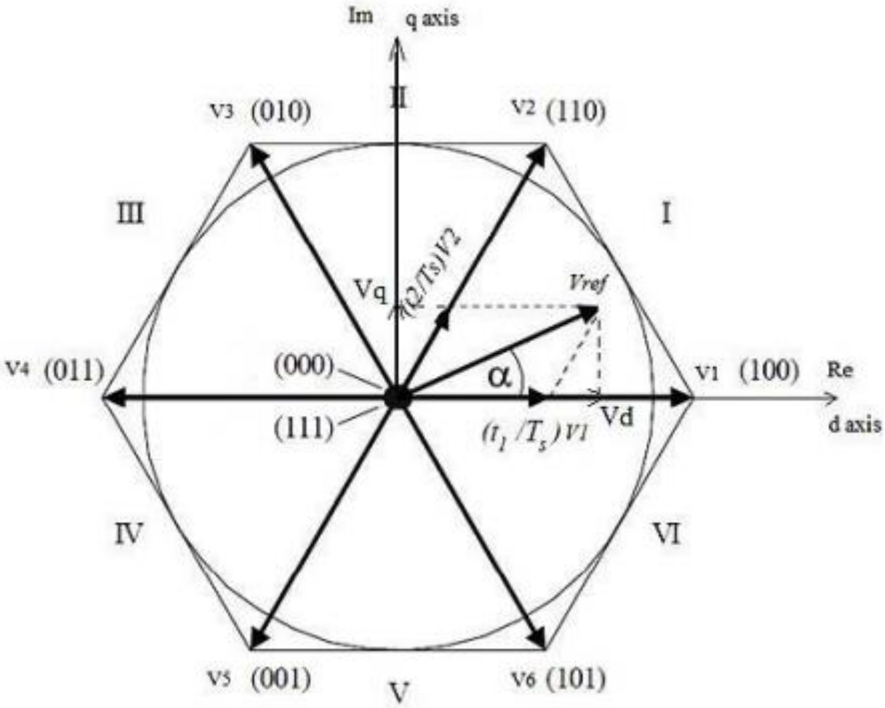

Figure 4.3 Voltage vector Vs based on switching states.(Ildarabadi and Ahmadi 2017)

The simple voltages V_{an}, V_{bn} and V_{cn} of the load derived from the compound voltages have a zero sum and are defined by:

$$\begin{cases} V_{an} = V_{n1} = \frac{1}{3}(U_{ab} - U_{ca}) \\ V_{bn} = V_{n2} = \frac{1}{3}(U_{bc} - U_{ab}) \\ V_{cn} = V_{n3} = \frac{1}{3}(U_{ab} - U_{bc}) \end{cases} \quad (4.1)$$

With,

$$\begin{cases} U_{ab} = V_{ano} - V_{bno} \\ U_{bc} = V_{bno} - V_{cno} \\ U_{ca} = V_{cno} - V_{ano} \end{cases} \quad (4.2)$$

It can be written as follow:

$$\begin{cases} V_{n1} = \frac{1}{3}(2V_{ano} - V_{bno} - V_{cno}) \\ V_{n2} = \frac{1}{3}(-V_{ano} + 2V_{bno} - V_{cno}) \\ V_{n3} = \frac{1}{3}(-V_{ano} - V_{bno} + 2V_{cno}) \end{cases} \tag{4.3}$$

However, the voltages delivered by the half-bridges are given by:

$$V_{ano} = \begin{cases} \frac{E}{2}\ if\ T_a\ is\ close \\ -\frac{E}{2}\ if\ T_a^{'}\ is\ close \end{cases} \tag{4.4}$$

$$V_{bno} = \begin{cases} \frac{E}{2}\ if\ T_b\ is\ close \\ -\frac{E}{2}\ if\ T_b^{'}\ is\ close \end{cases} \tag{4.5}$$

$$V_{cno} = \begin{cases} \frac{E}{2}\ if\ T_c\ is\ close \\ -\frac{E}{2}\ if\ T_c^{'}\ is\ close \end{cases} \tag{4.6}$$

Using the vector form of the voltages, we will have:

$$V_s = \sqrt{\frac{2}{3}}(V_{ano} + aV_{bno} + a^2V_{cno}) \tag{4.7}$$

With $a = e^{\frac{j2\pi}{3}}$

In other hand, we get:

$$V_{sno} = V_{an} + V_{bn} + V_{cn} \tag{4.8}$$

V_{sno}: is the voltage vector with reference to the midpoint of the inverter voltage.

V_s: is the voltage vector with reference to the neutral of the machine.

By introducing the logical variables of the state of the switches, the voltage vector can be written as:

$$V_s = \sqrt{\frac{2}{3}} * E * (S_a + aS_b + a^2 S_c) \tag{4.9}$$

E: The voltage supplied by the inverter.

If the load connected to the three-phase inverter is a balanced asynchronous motor, the phase voltages applied by the inverter to the motor stator are ($Van + Vbn + Vcn = 0$) and the phase-to-neutral voltages according to the switch states can be expressed as follows (Khlaief *et al*. 2011):

$$\begin{bmatrix} V_{an} \\ V_{bn} \\ V_{cn} \end{bmatrix} = \frac{E}{3} \begin{bmatrix} 2 & -1 & -1 \\ -1 & 2 & -1 \\ -1 & -1 & 2 \end{bmatrix} \begin{bmatrix} S_a \\ S_b \\ S_c \end{bmatrix} \tag{4.10}$$

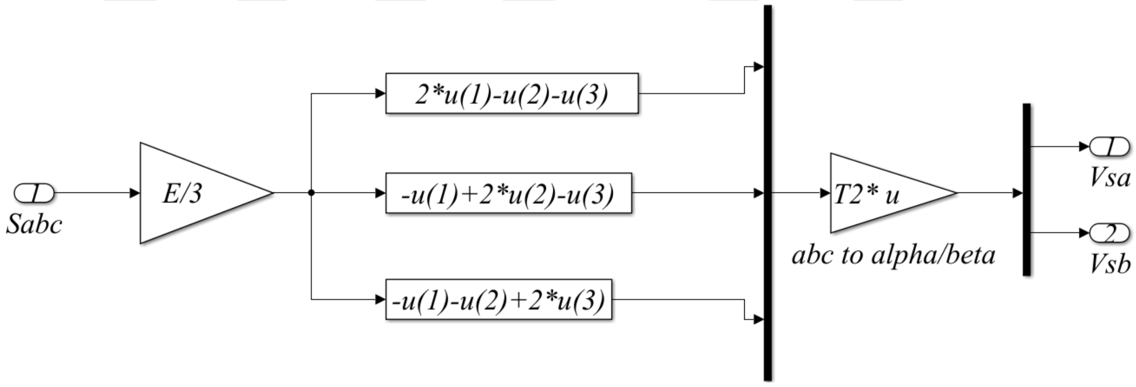

Figure 4.4 Represented voltage source inverter based on switch’s state on Simulink.

$$V_{sno} = V_s = V_{s\alpha} + jV_{s\beta} = \sqrt{\frac{2}{3}} * E * (S_a + aS_b + a^2 S_c) = \sqrt{\frac{2}{3}} * E * \left(S_a + S_b e^{\frac{j2\pi}{3}} + S_c e^{\frac{j4\pi}{3}}\right) \tag{4.11}$$

4.1.4 Torque vector control

The vector expressions of the machine in the stator reference frame are utilized:

$$\begin{cases} \overrightarrow{(V_s)} = R_s\overrightarrow{(I_s)} + \frac{d\overrightarrow{(\Phi_S)}}{dt} \\ \overrightarrow{(V_r)} = \vec{0} = R_r\overrightarrow{(I_r)} + \frac{d\overrightarrow{(\Phi_r)}}{dt} - j\sigma\overrightarrow{(\Phi_r)} \end{cases} \tag{4.12}$$

From the flux expressions, the rotor current is written:

$$\overrightarrow{(I_r)} = \frac{1}{\sigma}\left(\frac{\overrightarrow{(\Phi_r)}}{L_r} - \frac{L_m}{L_r\,L_s} * \overrightarrow{(\Phi_s)}\right) \tag{4.13}$$

With $\sigma = 1 - \frac{L_m^2}{L_r L_s}$

The expressions become

$$\overrightarrow{(V_s)} = R_s\,\overrightarrow{(I_s)} + \frac{d\overrightarrow{(\Phi_S)}}{dt} \tag{4.14}$$

$$\frac{d\overrightarrow{(\Phi_r)}}{dt} + \left(\frac{1}{\sigma\delta_r} - j\omega\right)\overrightarrow{(\Phi_r)} = \left(\frac{L_m}{L_s} * \frac{1}{\sigma\delta_r}\overrightarrow{(\Phi_s)}\right) \tag{4.15}$$

It shows us that:

The vector $\overrightarrow{(\Phi_s)}$ can be controlled from the vector $\overrightarrow{(V_s)}$ at the voltage drop $R_s\,\overrightarrow{(I_s)}$.

The flux $\overrightarrow{(\Phi_r)}$ follows the variations of $\overrightarrow{(\Phi_s)}$ with a period constant δ_r , the rotor acts as a filter of period constant $\sigma\delta_r$ between the fluxes $\overrightarrow{(\Phi_s)}$ and $\overrightarrow{(\Phi_r)}$.

In addition when reaches in steady state the expressions become as follow:

$$\overrightarrow{(\Phi_r)} = \frac{L_m}{L_s} * \frac{\overrightarrow{(\Phi_s)}}{1+j\omega\sigma\delta_r} \tag{4.16}$$

By putting ɣ = $\left(\overrightarrow{(\Phi_r)}, \overrightarrow{(\Phi_s)}\right)$ the electromagnetic torque can be expressed as:

$$\Gamma_{em} = p\frac{L_m}{\sigma L_r L_s}\Phi_s\Phi_r \sin ɣ \tag{4.17}$$

It can be observed that the torque depends on the amplitude of the two vectors $\overrightarrow{(\Phi_s)}$ and $\overrightarrow{(\Phi_r)}$ and their relative position.

If the flux Fs can be perfectly controlled from Vs in modulus and position, then the amplitude and relative position of Φ_s and thus the torque can be controlled. This is only possible if the switching period T_e is much smaller than $\sigma\delta_r$.

4.1.5 Stator flux control

Between two switching of the inverter switches, the selected voltage vector is always the same, hence:

$$\overrightarrow{(\Phi_s)} = \int_0^t \left(\overrightarrow{(V_s)} - R_s\,\overrightarrow{(I_s)}\right) dt \tag{4.18}$$

$$\overrightarrow{(\Phi_s)}(t) = \overrightarrow{(\Phi_s)}(0) + \overrightarrow{(V_s)} - \int_0^t R_s\,\overrightarrow{(I_s)}\,dt \tag{4.19}$$

If, for the purpose of simplification, we consider the voltage loss R I to be negligible compared to the voltage Vs , then we can see that in the interval [0,Te], the end of the vector FS moves on the straight line whose direction is given by the vector Vs selected during Te (Azib *et al*. 2016).

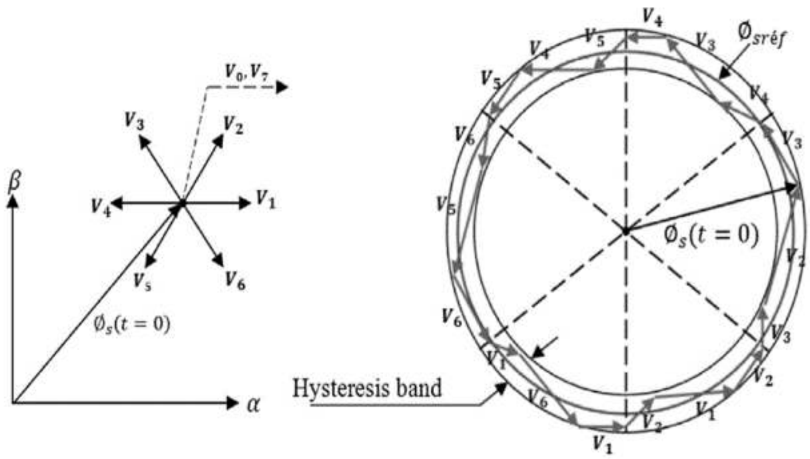

Figure 4.5 Trajectory of stator flux with the selected voltage vector Vs. (Zemmit, Messalti and Harag 2016).

4.1.6 Selecting the voltage vector vs

The choice of the vector Vs depends on the position of stator flux (***Φ***s) in the reference frame (α, β), the desired variation of its modulus, its sense of rotation and the variation of the torque.

The $\overrightarrow{(\Phi_s)}$ movement area is divided into six zones i, with i= [1;6].

When the flux is inside a zone i, flux and torque control can be achieved by selecting one of the following eight voltage vectors (Cheok and Fukuda 2002):

If V_{i+1} is chosen then $\overrightarrow{(\Phi_s)}$ increases and Γ_{em} increases.

If V_{i-1} is chosen then $\overrightarrow{(\Phi_s)}$ increases and Γ_{em} decreases.

If V_{i+2} is chosen then $\overrightarrow{(\Phi_s)}$ increases and Γ_{em} increases.

If V_{i-2} is chosen then $\overrightarrow{(\Phi_s)}$ decreases and Γ_{em} decreases.

If V_0 and V_7 are chosen then the rotation of stator flux is stopped and a drastic decreasing of Γ_{em} is shown taking into account the value of stator remains unchanged.

At the beginning of the region, the vectors V_{i+1} and V_{i-2} are perpendicular to $\overrightarrow{(\Phi_s)}$, which results in a rapid evolution of the torque but a slow evolution of the flux amplitude **Φ**s, whereas at the end of the region, the evolution is the opposite. With the vectors V_{i-1} and V_{i+2}, there is a slow evolution of the torque and a fast evolution of the amplitude Fs at the beginning of the zone, while at the end of the zone it is the opposite. The vectors V_i and V_{i+3} are not used whatever the direction of the torque or flux evolution because the flux component is very strong with a zero torque in the middle of the zone.

The voltage vector at the output of the inverter is deduced from the differences in torque and flux, estimated with respect to their reference, as well as the position of the vector Fs (Patel *et al*. 2011). A flux estimator in modulus and position as well as a torque estimator are therefore necessary.

4.1.7 Estimator

1) Estimator of stator flux

From the following expressions:

$$\overrightarrow{(\Phi_s)} = \int_0^t \left(\overrightarrow{(V_s)} - R_s \, \overrightarrow{(I_s)}\right) dt \qquad (4.20)$$

The stator current is measured while the stator voltage depends on the state of the switches (Sa, Sb, Sc), and on the DC link voltage Vdc (Bodkhe and Aware 2009). By projecting on the two axes α and β, we obtain the two components α and β of the estimated stator flux vector $\overrightarrow{(\Phi_s)}$, being:

$$\begin{cases} \overrightarrow{(\Phi_{s\alpha})} = \int_0^t \left(\overrightarrow{(V_{s\alpha})} - R_s \overrightarrow{(I_{s\alpha})}\right) dt \\ \overrightarrow{(\Phi_{s\beta})} = \int_0^t \left(\overrightarrow{(V_{s\beta})} - R_s \overrightarrow{(I_{s\beta})}\right) dt \end{cases} \quad (4.21)$$

As, $\overrightarrow{(\Phi_s)} = \overrightarrow{(\Phi_{s\alpha})} + j\overrightarrow{(\Phi_{s\beta})}$

In addition, by applying the transformation on the voltage we obtain:

$$V_{s\alpha} = \sqrt{\frac{2}{3}} * E * \left(S_a - \frac{1}{2}(S_b + S_c)\right) \quad (4.22)$$

$$V_{s\beta} = \frac{1}{\sqrt{2}} * E * (S_b - S_c) \quad (4.23)$$

$$V_s = V_{s\alpha} + jV_{s\beta} \quad (4.24)$$

Similarly, the currents $I_{s\alpha}$ and $I_{s\beta}$ are obtained from the measurement of the real currents Ia, Isb and Isc ($I_{sa} + I_{sb} + I_{sc} = 0$) and by applying the Clark transformation, we obtain:

$$I_{s\alpha} = \sqrt{\frac{2}{3}} * I_{sa} \quad (4.25)$$

$$I_{s\beta} = \frac{1}{\sqrt{2}} * (I_{sb} - I_{sc}) \quad (4.26)$$

$$I_s = I_{s\alpha} + jI_{s\beta} \quad (4.27)$$

The position and magnitude of the estimated stator flux are determined from the two flux components of the (α, β) frame, by:

$$\begin{cases} \overrightarrow{(\Phi_s)} = \sqrt{\Phi_{s\alpha}^2 + \Phi_{s\beta}^2} \\ \theta_s = atan2\left(\frac{\Phi_{s\beta}}{\Phi_{s\alpha}}\right) \end{cases} \quad (4.28)$$

The angle θ_s, which represents the position of the stator flux vector, allows us to determine the position of the flux vector.

2) Estimator of electromagnetic torque

The electromagnetic torque can be estimated from the estimated fluxes and measured currents, and can be expressed as follows:

$$\overrightarrow{(\Gamma_{em})} = \frac{3}{2} p \left(\overrightarrow{(\Phi_{s\alpha})} I_{s\beta} - \overrightarrow{(\Phi_{s\beta})} I_{s\alpha} \right) \quad (4.29)$$

In the Equation (4.29), it can be seen that the accuracy of the modulus of the electromagnetic torque depends on the quality of the flux estimation and the accuracy of the stator current measurement (El ouanjli *et al*. 2019).

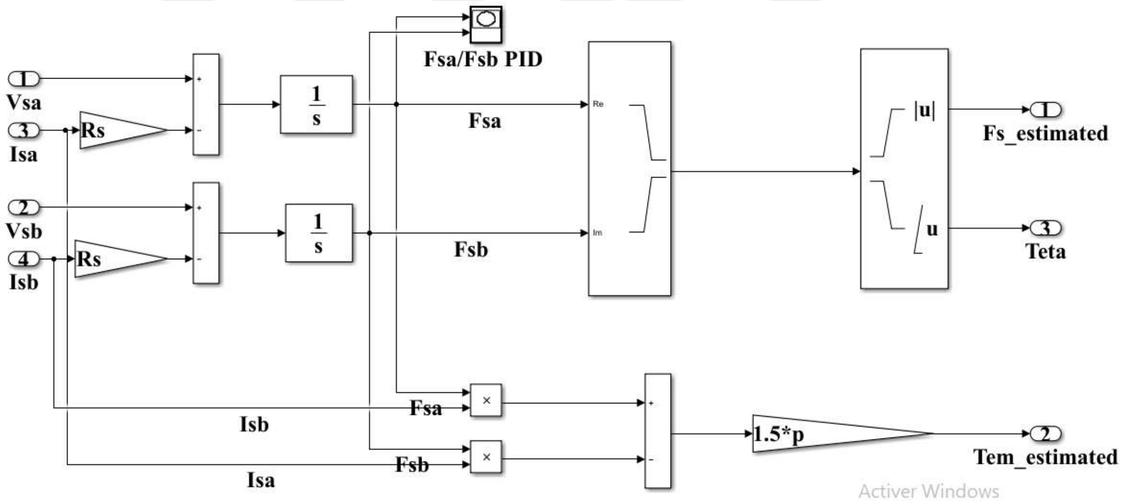

Figure 4.6 Stator flux and torque estimators block diagram represented on Simulink.

4.1.8 Hysteresis comparator

1) Flux hysteresis comparator

This comparator is simple in its use: its role is to maintain the end of the stator flux vector Φ_s in a circular band as shown in Figure 4.7. The error between the reference flux and the estimated flux is injected into the two-level hysteresis controller, which generates at its output the Boolean variable Φ_{flux}. This variable directly indicates whether the flux amplitude should be increased $(\Phi_{flux} = 1)$ or decreased $(\Phi_{flux} = 0)$ to keep the error between the estimated flux and the reference flux within a hysteresis width $\Delta\Phi_s$ and this expression $|\Phi_{ref} - \Phi_s| \leq \Delta\Phi_s$ must be checked. (Öztürk 2008)

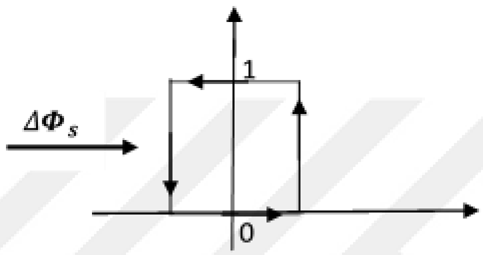

Figure 4.7 Structure of stator flux hysteresis corrector.

2) Torque hysteresis comparator

The main purpose of this electromagnetic torque comparator is to also keep the torque within the limits. The only difference with the flux comparator is that the electromagnetic torque can be positive or negative depending on the direction of rotation of the machine (Casadei *et al*. 2006). It is possible to propose two solutions (two-level or three-level comparator). The two-stage comparator allows controlling in one sense of rotation only, while the three-stage comparator can offer to control in case of inversion of the sense of rotation. It is strongly recommended to use in the torque, as the torque can be negative and positive at the same time.

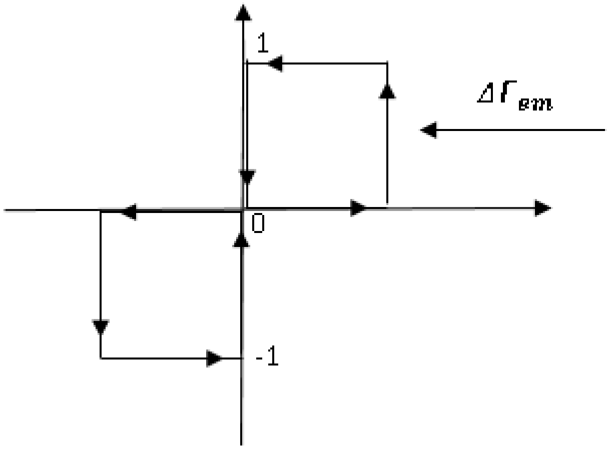

Figure 4.8 Structure of torque hysteresis comparator.

Here when it comes to represent on Simulink it gives us as follows:

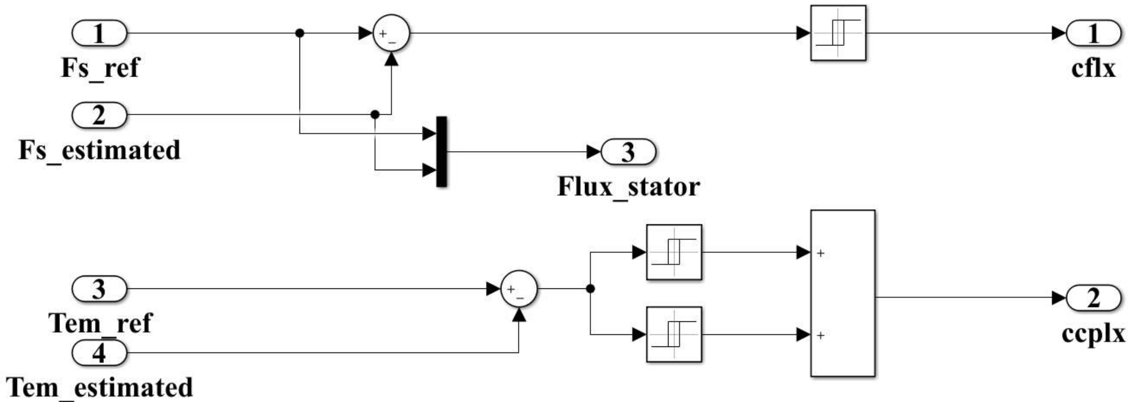

Figure 4.9 Flux and torque hysteresis comparator block diagram on Simulink.

4.1.9 Switching table

The switching table is created according to the state of the Boolean variables at the output of the two flux correctors and the electromagnetic torque, as well as the area giving the information on the position of the flux vector (Kumar, Thakur and Gupta 2014).

Table 4.1 Switching table for flux and torque correctors.

Flux	Torque	Sector 1	Sector 2	Sector 3	Sector 4	Sector 5	Sector 6
dΦ=1	dT=1	V_3	V_4	V_5	V_6	V_1	V_2
	dT=0	V_0	V_7	V_0	V_7	V_0	V_7
	dT=-1	V_5	V_6	V_1	V_2	V_3	V_4
dΦ=0	dT=1	V_2	V_3	V_4	V_5	V_6	V_1
	dT=0	V_7	V_0	V_7	V_0	V_7	V_0
	dT=-1	V_6	V_1	V_2	V_3	V_4	V_5

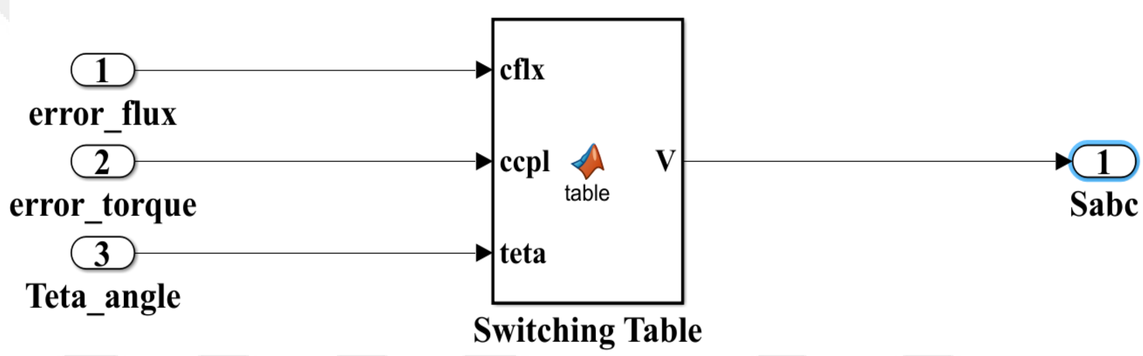

Figure 4.10 The switching table block diagram.

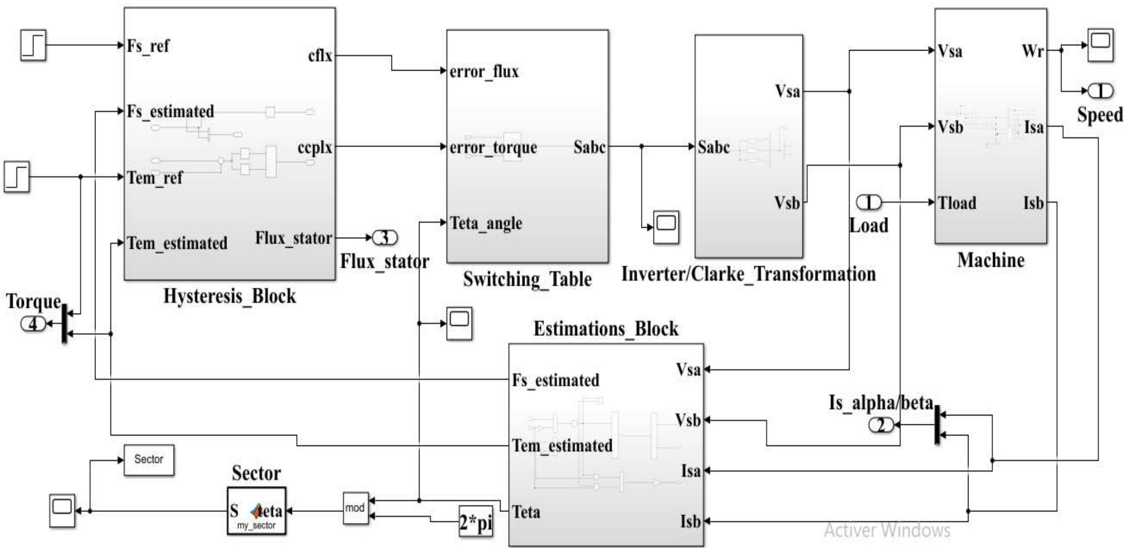

Figure 4.11 The conventional DTC represented on Simulink.

4.2 PI Applied On DTC of ASM

PID is widely used in industries to obtain performance on the systems to be controlled. Therefore, its main purpose is to regulate pressure, temperature, speed, flow, e.g. This controller requires a closed loop to control, providing a precise and stable response. The PID controller includes all of the necessary features, including a quick response to changes in the controller input, an increase in the control flag to reduce the error to zero, and reasonable activity inside the control blunder zone to eliminate motions. Subordinate mode improves the model system's soundness and allows for an increase in gain Kp, which increases the controller's reaction time. The mistake flag, the blunder vital, and the mistake subsidiary are the three terms that make up the PID controller's output (Abdullah and Ali 2020).

Because the integral term is present in the PI controller, the steady state error of speed is zero, making the system extremely accurate. It does not necessitate a high gain like a proportional gain controller does. However, there are certain disadvantages, such as the fact that if a very quick response is sought, the consequence paid is a greater overshoot, which is undesired. In the actual world, the PID controller seems to be a very effective approach to a variety of control problems (Aggarwal , Rai and Kandpal 2015).

The mathematical form of this controller can be described as follows:

$$U(t) = Kpe(t) + Ki\int_0^t e(\tau)d\tau + Kd\frac{de(t)}{dt} \qquad (4.30)$$

where Kp, Ki, and Kd are the coefficients for the proportional, integral, and derivative terms, respectively, and are all non-negative (sometimes denoted P, I, and D). but in our case we juste need for using PI (proportional and integral) instead of PID. Here the structure of used PI controller of motor drive can be shown below:

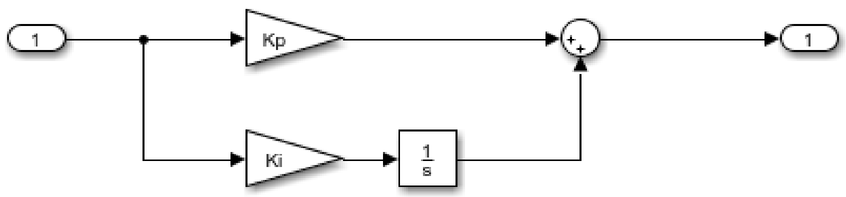

Figure 4.12 The structure of applied PI on motor drive.

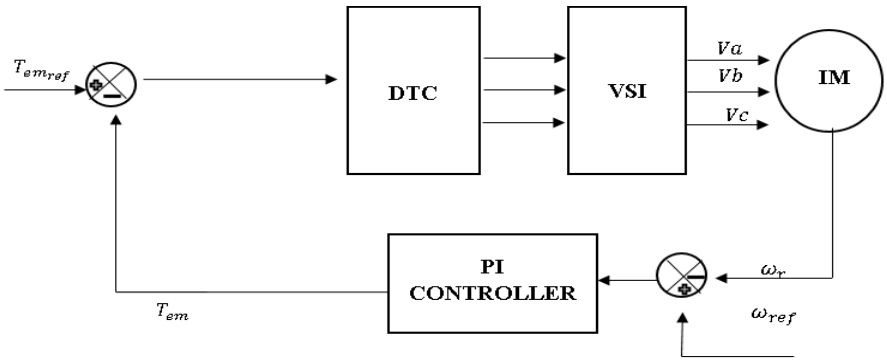

Figure 4.13 The design of PI controller applied on the motor.

4.3 Fuzzy Logic Controller

In contrast, to a standard controller or a state feedback controller, the fuzzy logic controller (FLC) does not deal with a well-defined mathematical relationship (Saad and Goléa 2017), but instead, it uses inferences with several rules, based on linguistic variables. In this section, we will present the general procedure of designing a fuzzy logic controller (Rambault 1993).

The basic configuration of a fuzzy logic controller has three main blocks:

- Fuzzyfication.
- Inference.
- Defuzzification.

The roles of each block can be described as follows:

1- The function of the fuzzification block is to establish the value ranges for the membership functions from the values of the input variables and perform a fuzzification function that converts the input data into suitable linguistic values (Bevrani and Daneshmand 2011).

2- The inference block is the central part of the FLC controller, which has the ability to simulate human decisions and to infer fuzzy control actions using fuzzy implication and inference rules (Mattavelli *et al*. 1997).

3- The defuzzification block also has the function of establishing the value ranges for the membership functions from the values of the output variables and performing a defuzzification that provides a non-fuzzy control signal from the derived fuzzy signal (Abdesselem 2008). We will go even further to understand the way they operate.

The fuzzy logic controller (FLC) is a sophisticated method controlling technology which reflects how humans make decisions. Scaling factors (SF), rule-base, and membership functions are the three basic components of the FLC speed controller (MFs). Preprocessing, processing, and post-processing are the three operational activities that make up FLC's system (Yordanova 2015). The input linguistic variables are turned (fuzzified) into fuzzy variables through input MFs during the pre-processing stage, which is known as fuzzification. The fuzzy rules are used for providing output fuzzy during the process. Through output MFs, the fuzzy output variable is turned (defuzzified) into a linguistic variable in the post-processing stage (Farah *et al*. 2021).

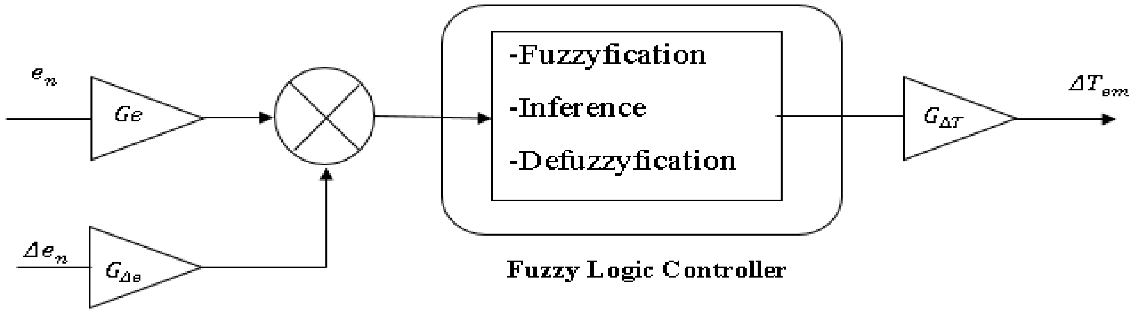

Figure 4.14 A block diagram of fuzzy speed controller.

a) Scaling Factors (SFs)

The scaling factor (SF) is a parameter gain that is being employed to normalize the value of a fuzzy variable. There are three SFs in the FLC speed controller: speed error SF (G_e), speed error's change SF ($G_{\Delta e}$), and output's change SF ($G_{\Delta T}$). The SF values typically pre-estimated depending on the motor's standard test conditions.

The variables representing the error, its change of speed and the change of output can be normalised as follows:

$$e_n = \frac{e}{G_e} \tag{4.31}$$

$$\Delta e_n = \frac{\Delta e}{G_{\Delta e}} \tag{4.32}$$

$$\Delta T_{em} = \frac{\Delta T_{em}}{G_{\Delta T}} \tag{4.33}$$

G_e, $G_{\Delta e}$, $G_{\Delta T}$ are gains that can be a constant or a variable . The right choice of these gains allows you to guarantee stability and improve the dynamic and static performance of the desired control.

b) Rules

The purposed fuzzy control scheme's fuzzy control rules are designed to reduce torque ripples, and the rules can be derived from the investigators' previous experience with the DTC system (Korkmaz *et al*. 2012)

A fuzzy rule-base is a collection of IF-THEN statements that determine the fuzzy output system depending on the input fuzzy state (Czabanski, Jezewski and Leski 2017). The rulebase for FLC speed control with two inputs (e_n, Δe_n) and one output (ΔT_{em}) is as follows:

If e_n is A and Δe_n is B then ΔT_{em} is C

Where the membership function names A, B, and C can be changed by negative large (NL), negative medium (NM), negative small (NS), zero (ZE), positive small (PS), positive medium (NM), and positive large (PL). There are three different standard rule-base for controlling speed on induction motor (IM) in FLC. A rule base 3x3, 5x5 and 7x7 will be illustrated in the Table 4.2, 4.3, 4.4 below.

Table 4.2 Rule-base 3x3 table.

e_n \ Δe_n	NL	ZE	PL
NL	NL	NL	ZE
ZE	NL	ZE	PL
PL	ZE	PL	PL

Table 4.3 Rule-base 5x5 table.

e_n \ Δe_n	NL	NS	ZE	PS	PL
NM	NL	NL	NL	NS	ZE
NS	NL	NL	NS	ZE	PS
ZE	NL	NS	ZE	PS	PL
PS	NS	ZE	PS	PL	PL
PL	ZE	PS	PL	PL	PL

Table 4.4 Rule-base 7x7 table.

e_n \ Δe_n	NL	NM	NS	ZE	PS	PM	PL
NL	NL	NL	NL	NL	NM	NS	ZE
NM	NL	NL	NL	NM	NS	ZE	PS
NS	NL	NL	NM	NS	ZE	PS	PM
ZE	NL	NM	NS	ZE	PS	PM	PL
PS	NM	NS	ZE	PS	PM	PL	PL
PM	NS	ZE	PS	PM	PL	PL	PL
PL	ZE	PS	PM	PL	PL	PL	PL

c) Membership functions

The range of the fuzzy variable is represented graphically by membership functions (MFs). Based on the amount of MFs utilized, it breaks the range into distinct widths. There are various sorts of MFs in terms of shape, namely triangular, trapezoidal, sigmoidal, Gaussian, Z-shape, and S-shape MFs. Due to their great precision and low processing complexity, triangular and trapezoidal MFs are the most often utilized MFs in FLC speed control. Just triangular MFs will indeed be addressed in this thesis, and the centroid algorithm will be employed as a fuzzification tool. 3x3, 5x5, and 7x7 MFs are the three most common triangle MF sizes. The shape of these MFs will be as illustrated in Figure below. If their breadth and location are symmetrically designed. The breadth and MFs's position are symmetrical, with the width between each MF being evenly distributed. The existing MFs's shape is referred to as standard MFs, but modifying the breadth and peak location of MFs effectively can improve the drive system's performance (Farah *et al*. 2021).

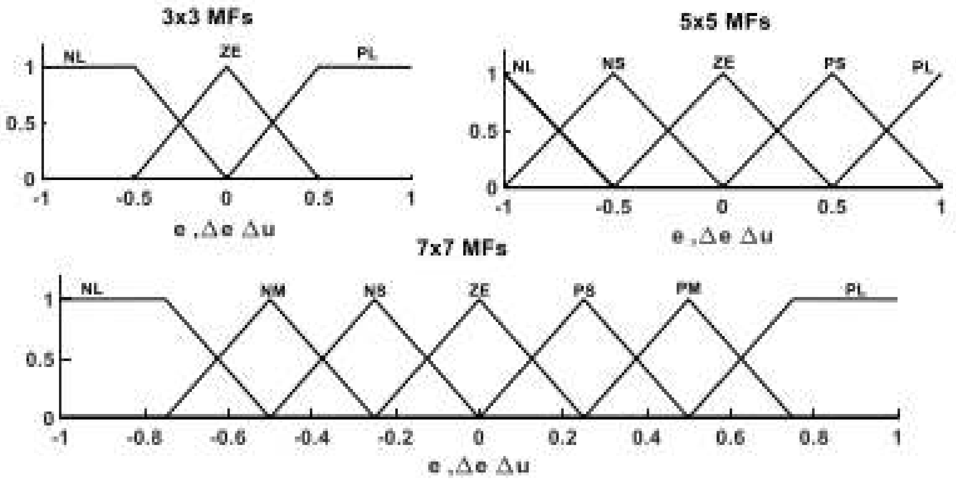

Figure 4.15 Membership function of inputs and outputs.

After having briefly explained the controller, we are planning to choose in this thesis rule-base 7x7 table and 7x7 of the membership function to be done in matlab. Here is the figure shown below

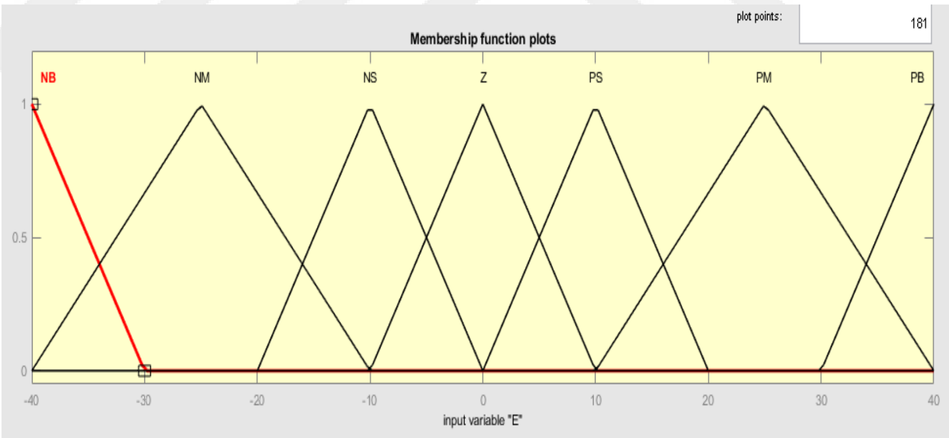

Figure 4.16 Membership function of input E.

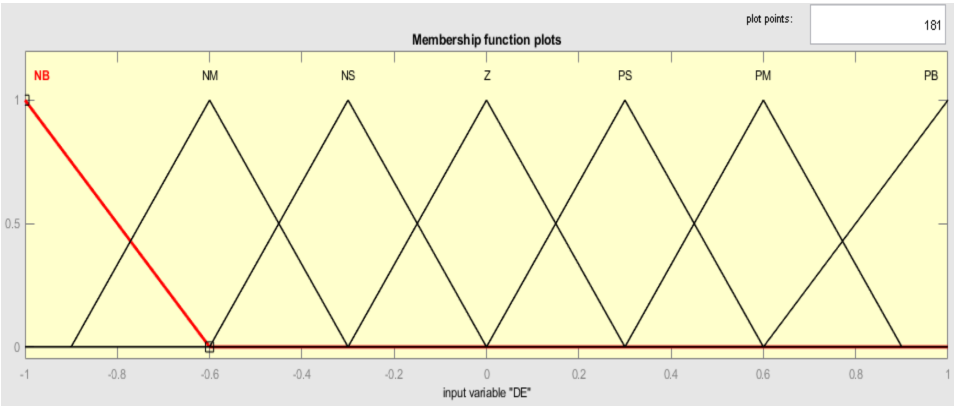

Figure 4.17 Membership function of input DE.

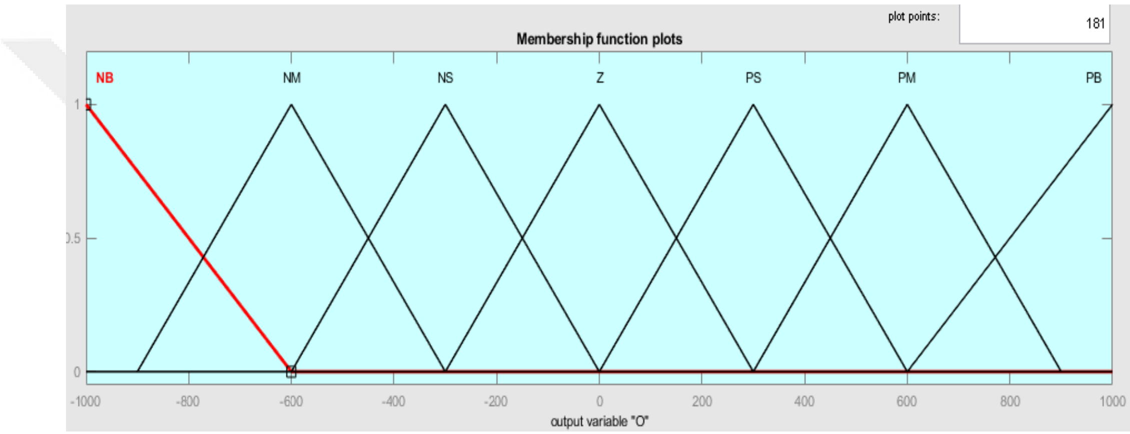

Figure 4.18 Membership function of output.

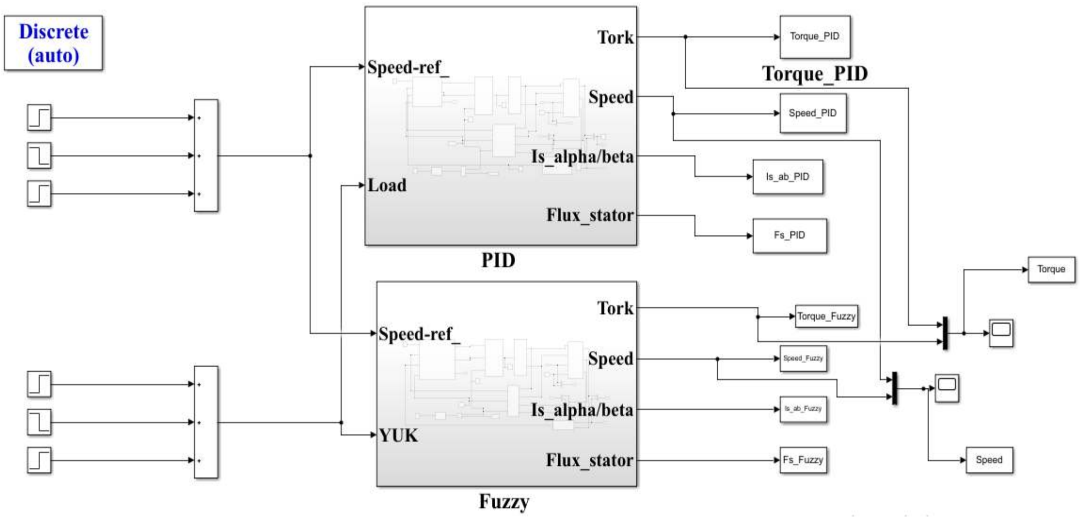

Figure 4.19 PID and fuzzy logic regulators represented on Simulink.

5. RESULTS AND DISCUSSION

a. For voltage source

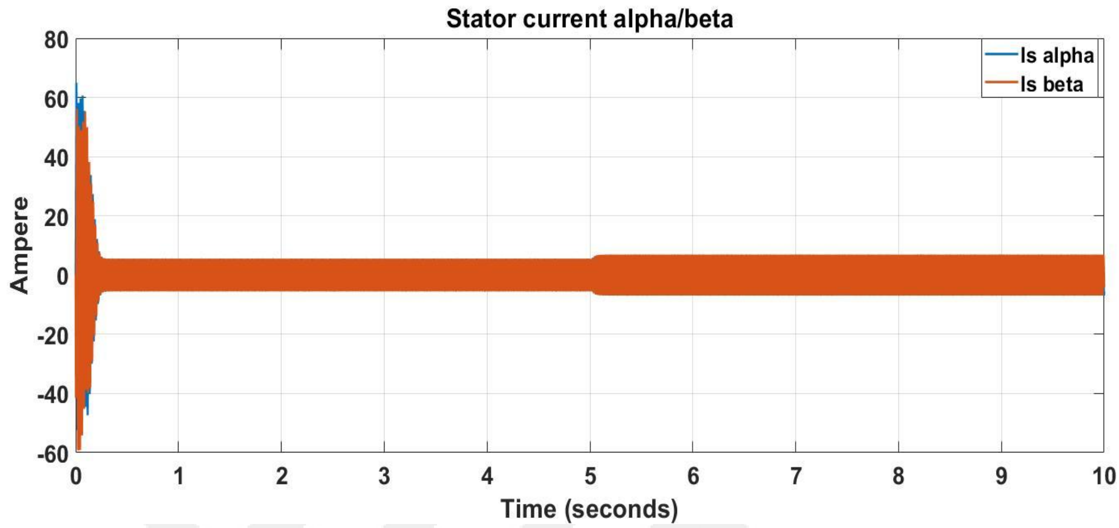

Figure 5.1 Stator current's result after being simulated in Simulink.

This illustration shows the stator current represented in α-β region under direct voltage supply. At start-up, it is visible that there has been a large current demand and gradually the graph starts to stabilize. At time t=5 s, a load has been applied to the motor. Then it requires a not too bad current for the rest of the simulation. We can therefore say that the current is large at start-up and stabilizes with time but when the load is large, it will demand a large amount of current resulting in increased energy consumption.

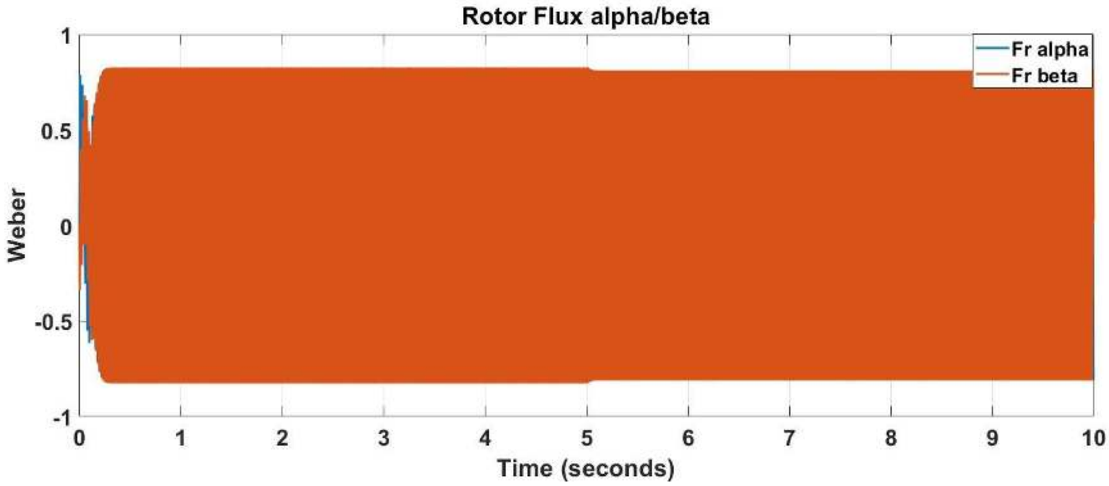

Figure 5.2 Rotor flux's result.

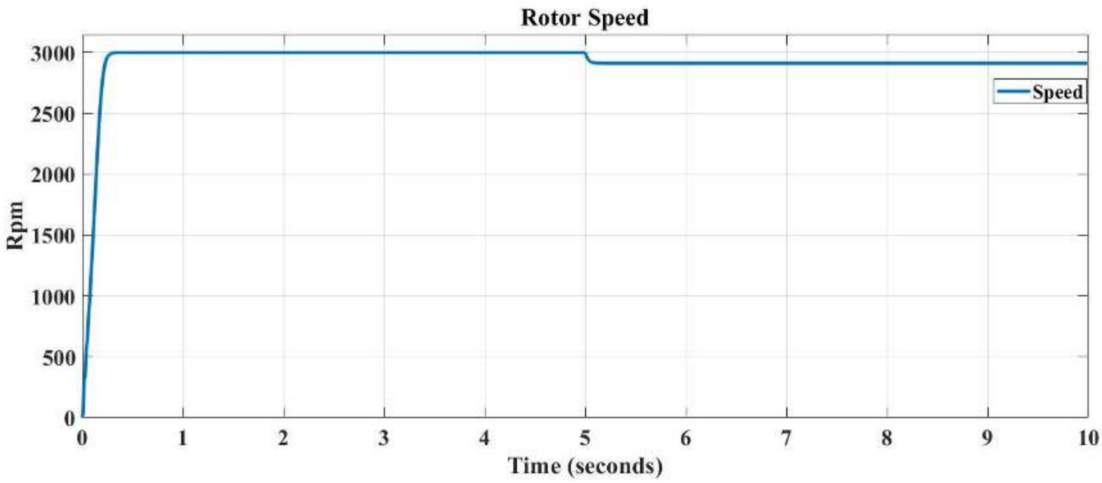

Figure 5.3 Rotor speed's result.

According to this graph, the desired speed is obtained when the power supply is tried. At time t=5 s, a load is applied to the machine and the speed starts to decrease. To provide a better performance to the machine and to be able to control the speed, we will then propose an advanced method using the regulators discussed above.

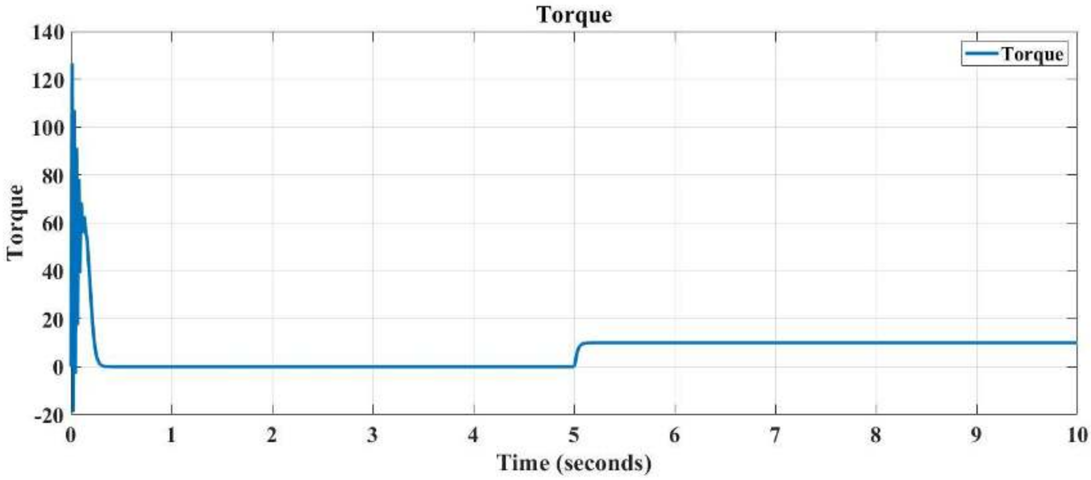

Figure 5.4 Torque's result simulation on Simulink.

The torque is also visualized. We can see that at start up it had a lot of torque demand and as time went by it started to stabilize. Then a not so important load is applied, T=25 Nm, and we could obtain the desired torque.

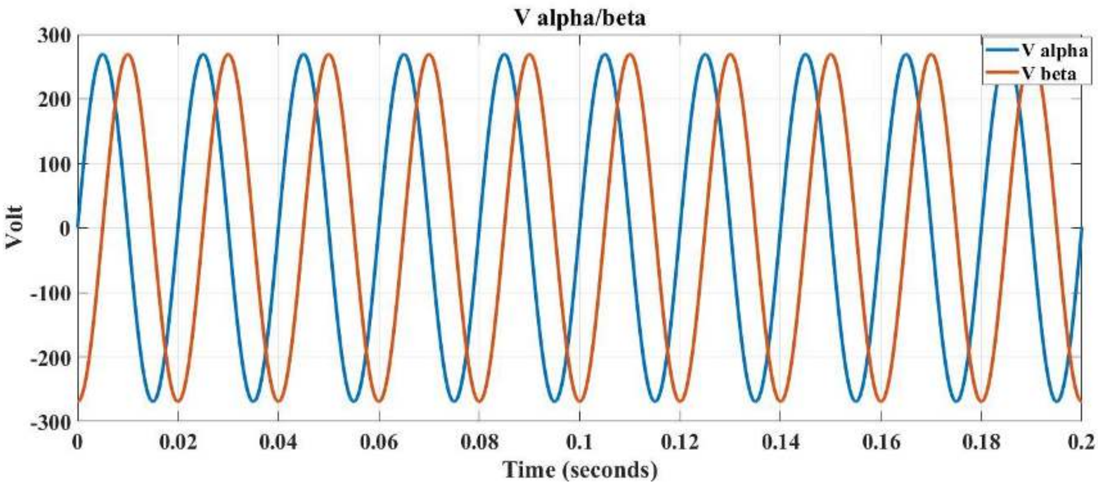

Figure 5.5 Voltage alpha-beta's result on Simulink

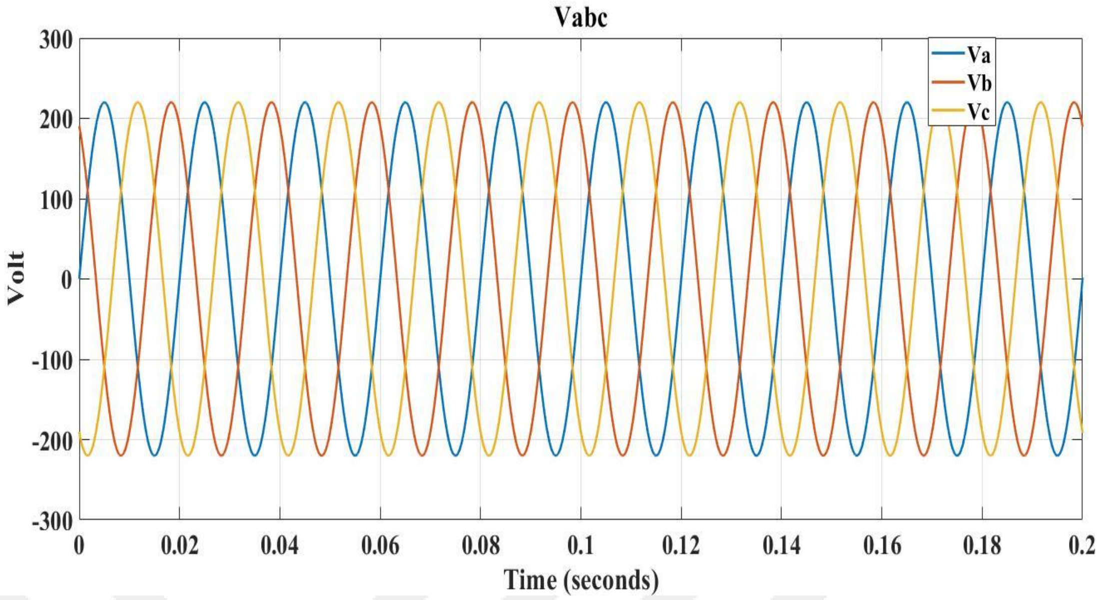

Figure 5.6 The output of three-phase abc voltage source.

b. For conventional DTC

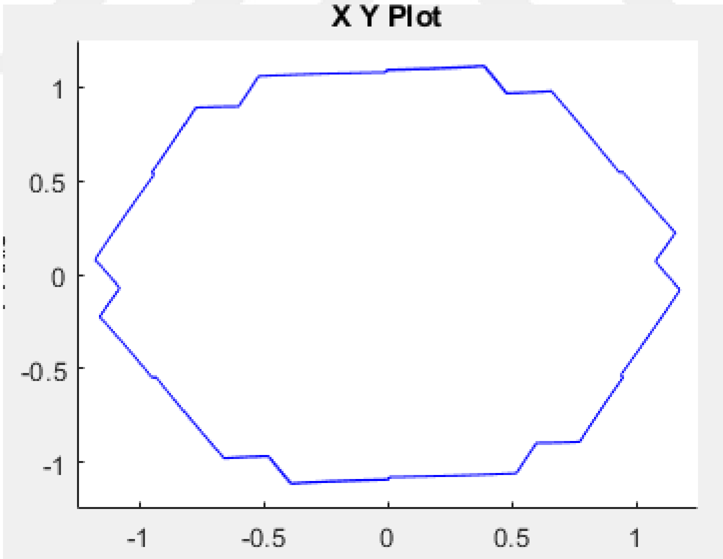

Figure 5.7 Trajectory of stator flux alpha-beta frame.

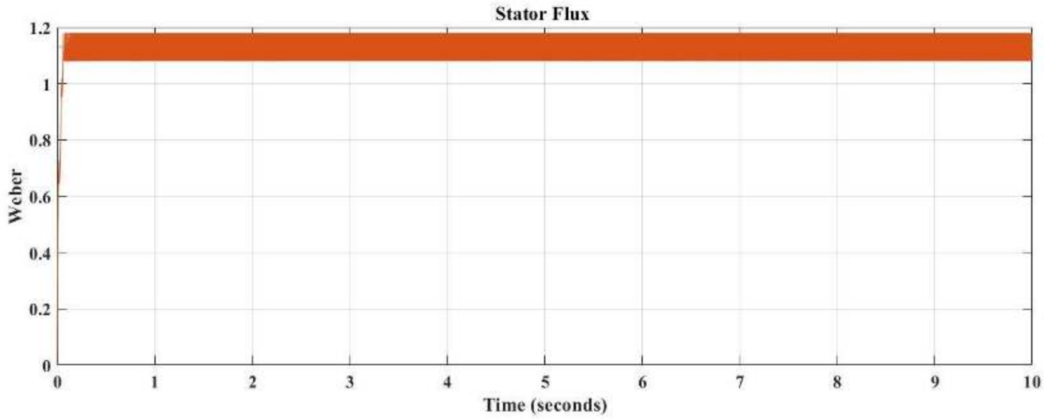

Figure 5.8 Stator flux's result

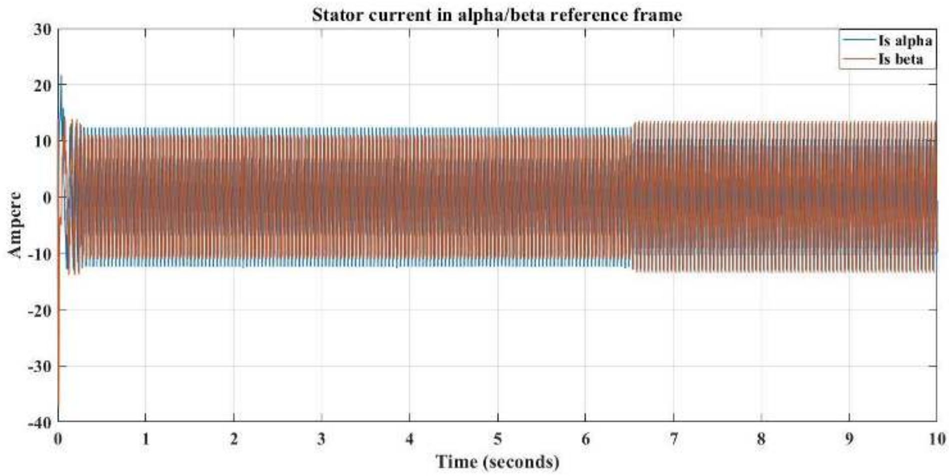

Figure 5.9 Stator current's response in alpha-beta reference frame.

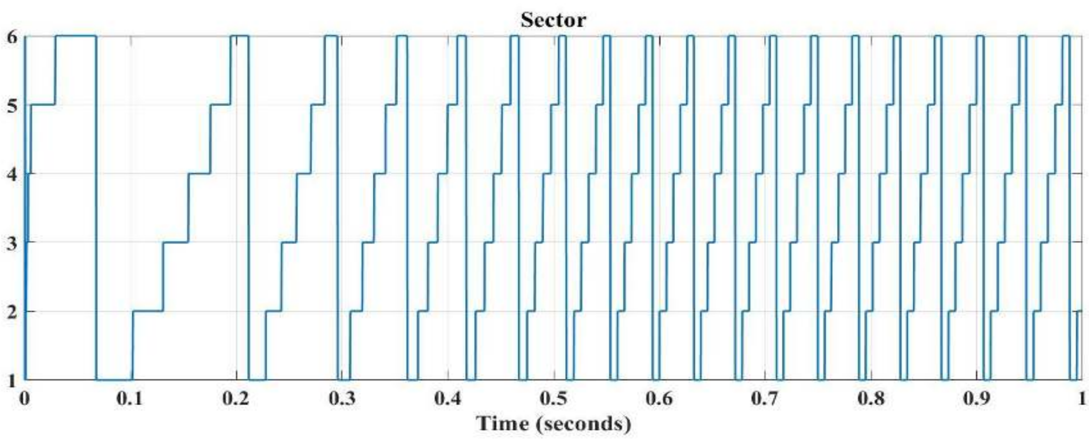

Figure 5.10 Sector's result.

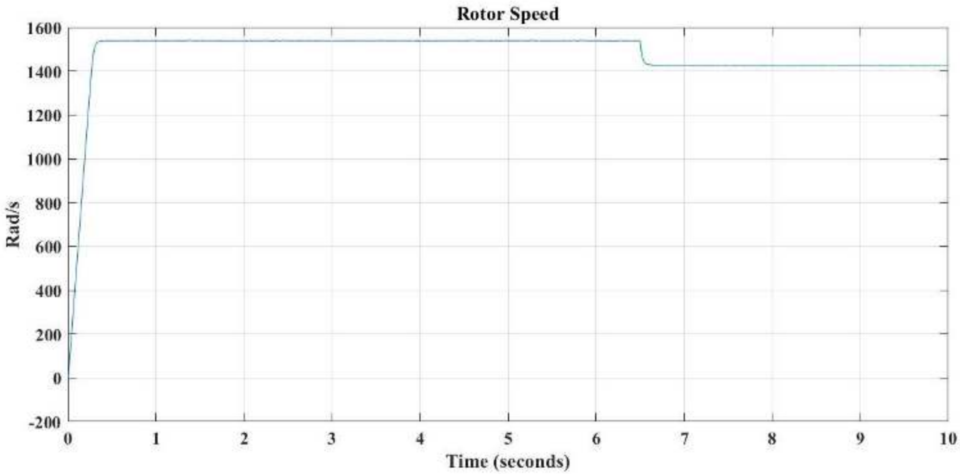

Figure 5.11 Rotor speed's result.

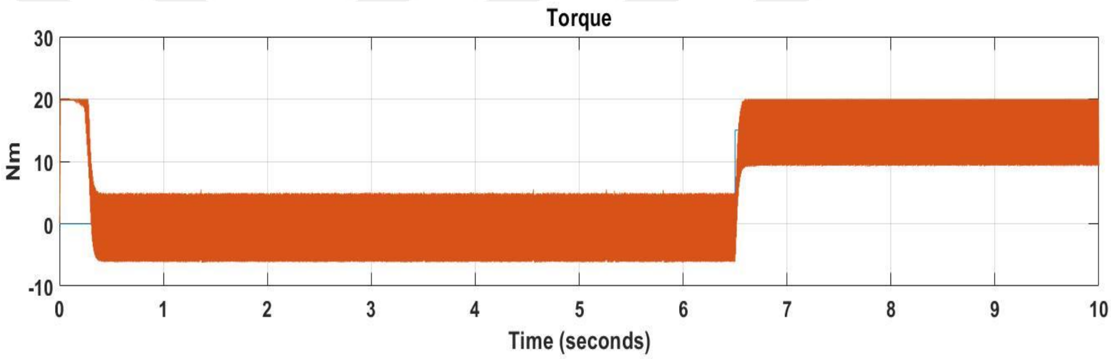

Figure 5.12 Torque's response

The objective of the direct torque control is to provide us with a control at the level of the torque which has been estimated from the estimator block. We have managed to control it, but the response of the rotor speed is questionable. We notice that here the response is too slow. In the classic DTC method without the regulators, there is likely to be a slowdown in the response of the system and the speed is not controlled as well as the torque. In the subsequent result using the regulators, we will see a much faster response than the DTC method. For that, we are going to propose an advanced method like the fuzzy logic controller and the PI, which are going to start to control the speed and to provide us with a much faster response than the classic direct torque control.

c. Fuzzy and PI results

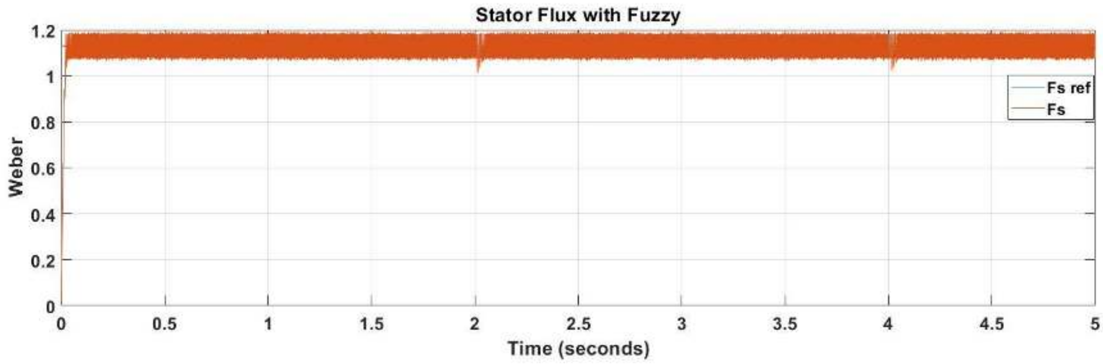

Figure 5.13 Stator flux’s response with fuzzy logic regulator on Simulink.

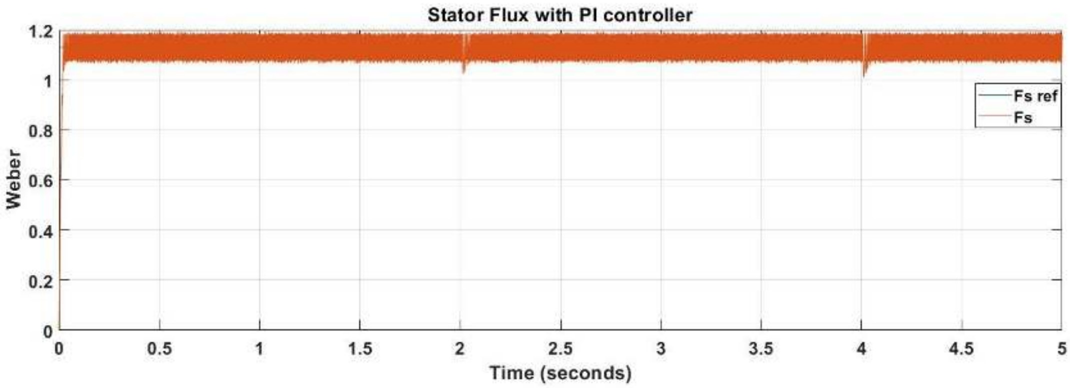

Figure 5.14 Stator flux’s result with PI regulator.

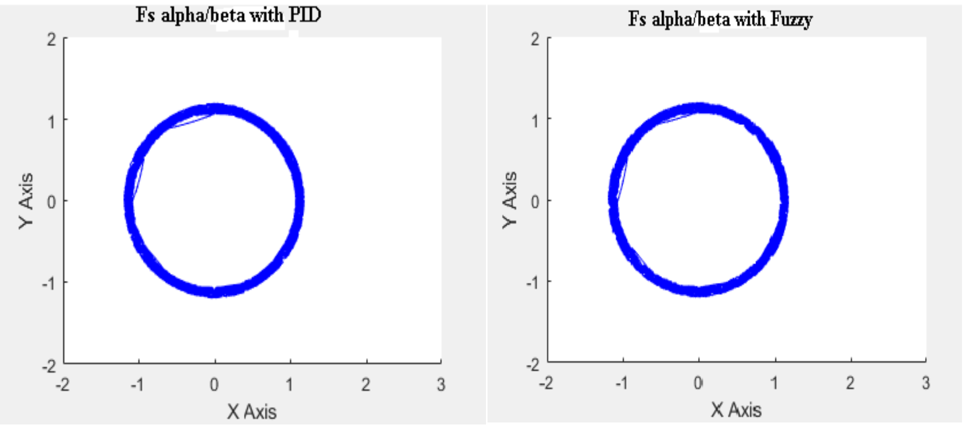

Figure 5.15 Stator flux with PI and fuzzy logic controller in alpha-beta frame.

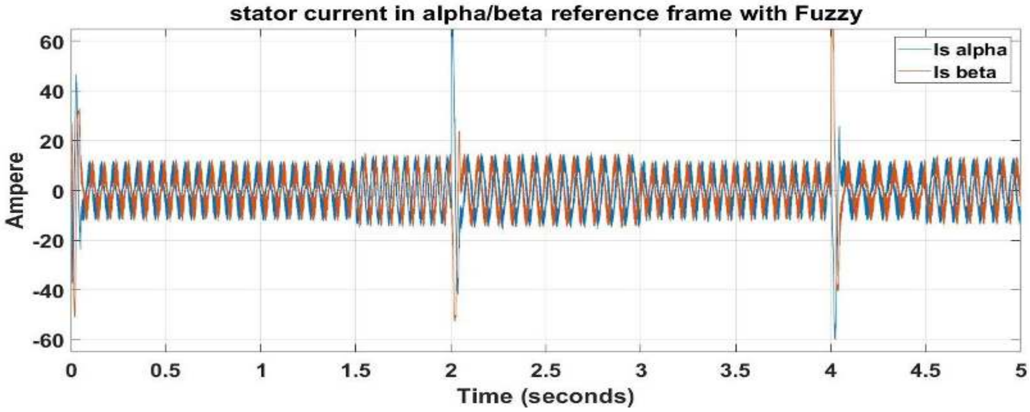

Figure 5.16 Stator current' response in alpha-beta frame using fuzzy logic controller.

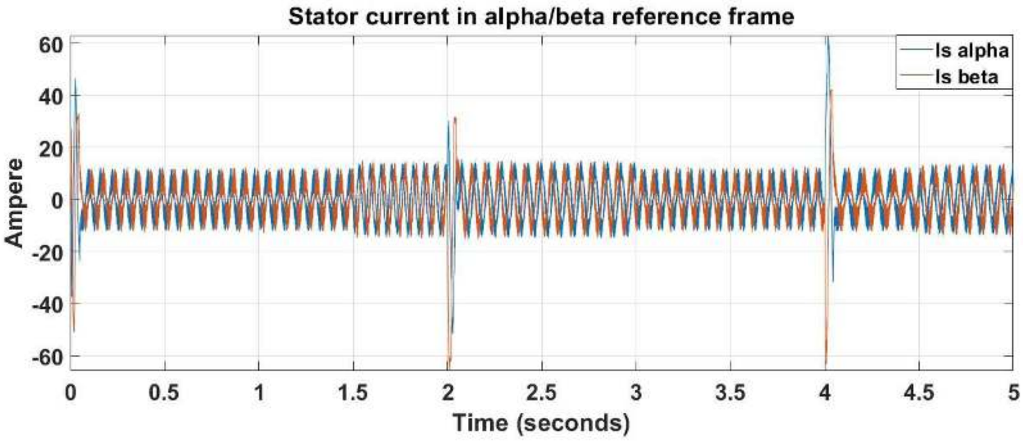

Figure 5.17 Stator current'result in alpha-beta frame using PI controller.

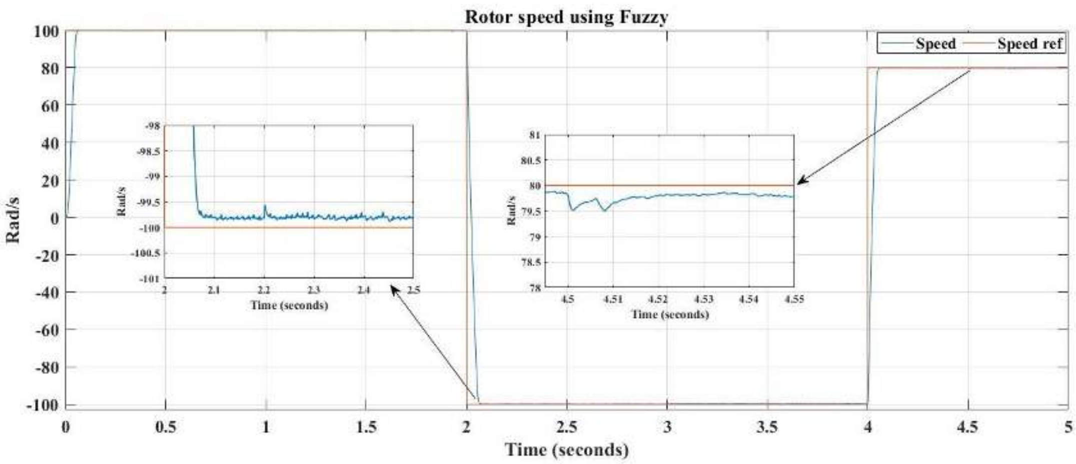

Figure 5.18 Speed's response by using Fuzzy logic controller.

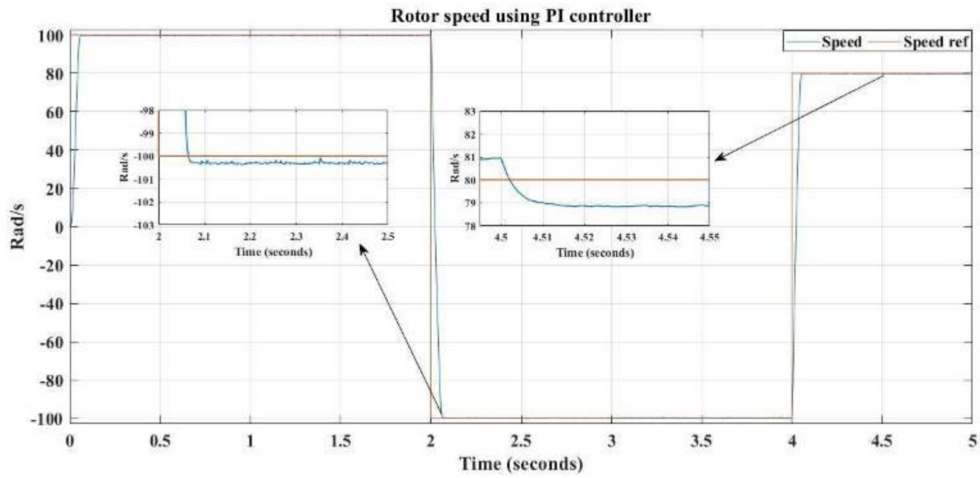

Figure 5.19 Speed's response using PI regulator.

The direction of inversion of the motor was also carried out in order to get as much information as possible about the response to this situation. To begin with, Both methods showed excellent response at start-up, but when the speed reference was changed, the fuzzy logic showed excellent performance not only in tracking the reference point but also when a change in torque reference was modified, it also showed excellent response, as you can see in the Figure 5.19. In terms of efficiency and responsiveness, the fuzzy logic clearly outperforms the PI regulator.. Indeed, when we focus on the exceeding, the PI slightly exceeds the set point, which could affect the performance of the machine whereas the fuzzy logic tries as fast as possible to reach the set point.

When there has been a reversal of the direction of rotation at time t=2 s and t=4 s, the fuzzy logic gives a good impression in response unlike the PI controller.

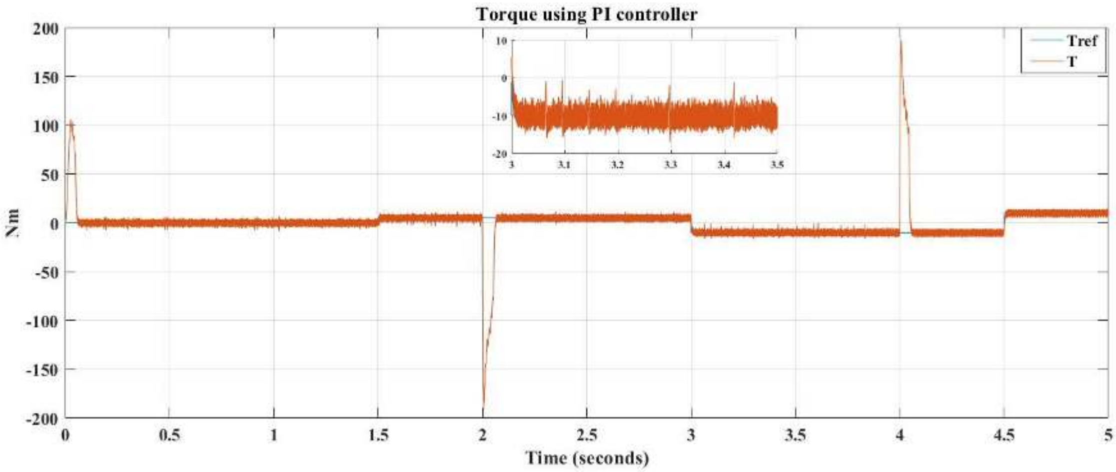

Figure 5.20 Torque’s response with the use of PI controller.

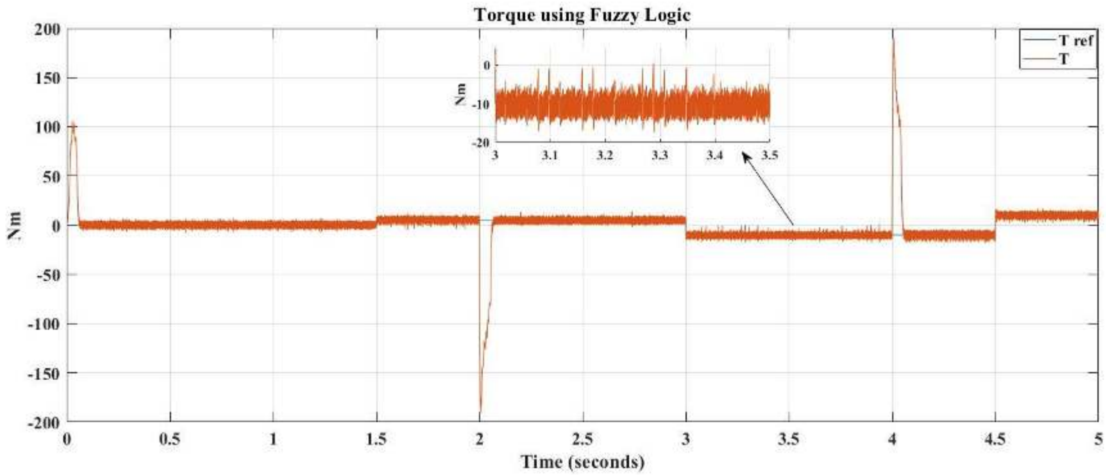

Figure 5.21 Torque’s result with the use of fuzzy logic controller.

At start-up it is very noticeable that the torque is high. both controllers brought a lot of improvement in the reduction of the torque ripple at start-up. At t= 1.5 to t=2, The fuzzy logic method has slightly reduced the torque ripple in contrast to the PI regulator, as shown in the figure. However, both of them shows a slight ripple when the torque becomes negative.

6. CONCLUSIONS AND RECOMMENDATION

The aim of this work is not only to justify our choice of control strategy, but also to show the contribution of our study to the subject. Thus, in a first step, we have detailed the model of the three-phase asynchronous machine and the type of power supply considered. Then, we considered the principle of direct torque control in its classical variant, more and more used in industrial environments. However, often criticized and unable to meet the new constraints imposed by some industries where high performances and high dynamics are required such as: a good fast tracking for the speed and a reduced ripple rate for the torque and the flux.

The control of the main parameters of the asynchronous machine, namely the stator flux and the electromagnetic torque, is achieved by direct selection of the output voltage vectors of the inverter from a switching table. These choices are made in such a way that they can keep both quantities in a hysteresis band in the range of their reference values. However, the existence of hysteresis controllers in the conventional direct torque control strategy generates torque and flux oscillations due to the bandwidth of the hysteresis controllers. Thus, since our study is mainly concerned with the minimization of the ripple of the electromagnetic torque and stator flux of the direct torque control applied to the three-phase induction machine.

In the previous section, the principles of fuzzy logic control and PI controller have been introduced and our choice of these methods for controlling asynchronous machines has been justified. Then, the design aspects of a fuzzy FLC controller for the speed control and PID controllers loop were presented. After selecting the Simulink simulation method and confirming its efficiency, we used this simulation under several operating conditions in order to rigorously exploit the different results that we obtained. After the comparison, we can state that fuzzy logic outperforms the PI controller in term of effectiveness, responsiveness and robustness.

The majority of researchers have decided to suggest that the best way to further reduce the ripple at the torque level is to put a pi at the comparator and replace the switching table with a fuzzy table. Moreover, others have tried other fuzzy similar methods such as artificial neuron and genetics. It has allowed them to have a significant result. If it will be possible for me to continue to the PhD degree, I will take a similar subject related to artificial intelligence for my Phd degree.

REFERENCES

Abdesselem, C. 2008. Commande directe du couple du moteur asynchrone-apport de la logique floue. Msc. Thesis, Batna University, 105 pages, Algeria.

Abdullah, A. N., and Ali, M. H. 2020. Direct torque control of IM using PID controller. *International Journal of Electrical and Computer Engineering*, *10*(1), 617.

Aggarwal, A., Rai, J. N., and Kandpal, M. 2015. Comparative study of speed control of induction motor using pi and fuzzy logic controller. *IOSR Journal of Electrical and Electronics Engineering (IOSR-JEEE)*, *10*(2), 43-52.

Azib, A., Ziane, D., Rekioua, T., and Tounzi, A. 2016. Robustness of the direct torque control of double star induction motor in fault condition. *Rev. Roum. Sci. Techn. Électrotechn. et Énergn*, *61*(2), 147-152.

Benzaioua, A. 2014. Contribution à la commande directe de couple d'une machine asynchrone triphasée. PhD. Thesis, Québec à Chicoutimi University, 163 pages, Québec.

Bevrani, H., and Daneshmand, P. R. 2011. Fuzzy logic-based load-frequency control concerning high penetration of wind turbines. IEEE systems journal, 6(1), 173-180.

Bodkhe, S. B., and Aware, M. V. 2009. Speed-sensorless, adjustable-speed induction motor drive based on dc link measurement. *International Journal of Physical Sciences*, *4*(4), 221-232.

Brown, D. W., Abbas, M., Ginart, A., Ali, I. N., Kalgren, P. W., and Vachtsevanos, G. J. 2011. Turn-off time as an early indicator of insulated gate bipolar transistor latch-up. *IEEE Transactions on Power Electronics*, *27*(2), 479-489.

Bulut, A. 2019. Doğrudan moment kontrolünde kalman filtresi uygulaması. Yüksek Lisans Tezi, İstanbul Ünıversitesi, 65 sayfa, İstanbul.

Can, E., and Sayan, H. 2016. PID and fuzzy controlling three phase asynchronous machine by low level DC source three phase inverter. Tehnicki Vjesnik-Technical Gazette, 23(3).

Casadei, D., Serra, G., Tani, A., and Zarri, L. 2006. Assessment of direct torque control for induction motor drives. Bulletin of the Polish Academy of Sciences: Technical Sciences, 237-254.

Cheok, A. D., and Fukuda, Y. 2002. A new torque and flux control method for switched reluctance motor drives. *IEEE Transactions on Power Electronics*, *17*(4), 543-557.

Circuit Globe, 2022. Web site. https://circuitglobe.com/category/electrical-terms/electrical-machines/induction-motor. Date of access: 04.05.2022

Czabanski, R., Jezewski, M., and Leski, J. 2017. Introduction to fuzzy systems, Theory and Applications of Ordered Fuzzy Numbers. Prokopowicz, P and et al. (eds), Springer Open, pp. 38-43, Poland.

DESIGNSPARK, 2016. Web site. https://www.rs-online.com/designspark/different-types-of-motors-and-their-use. Date of access.05.04.2022.

El ouanjli, N., Derouich, A., El Ghzizal, A., Bouchnaif, J., El Mourabit, Y., Taoussi, M., and Bossoufi, B. 2019. Real-time implementation in dSPACE of DTC-backstepping for a doubly fed induction motor. *The European Physical Journal Plus*, *134*(11), 1-14.

Electrical 4 U. Web site. https://www.electrical4u.com/torque-slip-characteristics-of-induction-motor. Date of access: 09.04.2022.

Ellabban, O., Van Mierlo, J., and Lataire, P. 2011. A comparative study of different control techniques for an induction motor fed by a Z-source inverter for electric vehicles. *International Conference on Power Engineering, Energy and Electrical Drives* (pp. 1-7). IEEE.

El-Shimy, M. E., and Zaid, S. A. 2016. Fuzzy PID controller for fast direct torque control of induction motor drives. Journal of Electrical Systems, 12(4), 687-700.

Farah, N., Talib, H. N., Ibrahim, Z. B., Abdullah, Q., Aydoğdu, Ö., Lazi, J. M., and Isa, Z. 2021. Fuzzy membership functions tuning for speed controller of induction motor drive: Performance improvement. *Indonesian Journal of Electrical Engineering and Computer Science*, *23*(3), 1258-1270.

Ghani, A., Tahour, A., Colak, I. 2018. Introduction to the design and the control of electrical machines, Optimization and Control of Electrical Machines, Algeria.

Hu, J., Nian, H., Hu, B., He, Y., and Zhu, Z. Q. 2010. Direct active and reactive power regulation of DFIG using sliding-mode control approach. *IEEE Transactions on energy conversion*, *25*(4), 1028-1039.

Ildarabadi, R., and Ahmadi, A. 2017. Simulation Study of Space Vector Pulse Width Modulation Feeding a Three Phase Induction Motor.

Khlaief, A., Jemli, K., Boussak, M., and Gossa, M. 2011. Study on inverter's IGBT fault behavior with permanent magnet synchronous motor's drive. *Analysis and Implementation of Single-Stage Interleaved Double Buck-Boost Converter with High Power Factor*, 1581.

Korkmaz, F. 2016. A new approach to dtc method for bldc motor adjustable speed drives. In The Fourth International Conference on Instrumentation and Control Systems (CICS-2016) (Vol. 6, No. 5).

Korkmaz, F., Çakır, M. F., Korkmaz, Y., and Topaloğlu, I. 2012. Fuzzy based stator flux optimizer design for direct torque control. arXiv preprint arXiv:1212.0160.

Korkmaz, F., Topaloğlu, İ., and Mamur, H. 2015. Fuzzy logic based direct torque control of induction motor with space vector modulation. arXiv preprint arXiv:1508.01345.

Kumar, D., Thakur, I., and Gupta, K. 2014. Direct torque control for induction motor using intelligent artificial neural network technique. *International Journal of Emerging Trends & Technology in Computer Science (IJETTCS)*, *3*(4), 44-50.

Mattavelli, P., Rossetto, L., Spiazzi, G., and Tenti, P. 1997. General-purpose fuzzy controller for DC-DC converters. *IEEE transactions on Power Electronics*, *12*(1), 79-86.

Mevey, J.R. 2006 Sensorless field oriented control of brushless permanent magnet synchronous motors. Msc. Thesis, B.S, Kansas State University, 355 pages, United States.

Microsemi 2013. Web site. https://www.microsemi.com/document-portal/doc_view/132799-park-inverse-park-and-clarke-inverse-clarke-transformations-mss-software-implementation-user-guide. Date of access: 10.02.2022

Ötkün, Ö. 2020. Scalar speed control of induction motors with difference frequency. *Journal of Polytechnic*, 23(2): 267-276.

Öztürk, S.B. 2008. Direct torque control of permanent magnet synchronous motors with non-sinusoidal back-emf. PhD. Thesis, Texas A&M University, 195 pages, United States.

Patel, C., Rajeevan, P. P., Dey, A., Ramchand, R., Gopakumar, K., and Kazmierkowski, M. P. 2011. Fast direct torque control of an open-end induction motor drive using

12-sided polygonal voltage space vectors. *IEEE Transactions on Power Electronics*, *27*(1), 400-410.

Popescu, M. 2000. Induction motor modelling for vector control purposes. Report, Helsinki University of Tehnology, 143 pages, Helsinki.

Proccessing, 2022. Web site. https://www.processingmagazine.com/pumps-motors-drives/article/15586862/the-dc-motor-advantage. Date of access: 02.04.2022.

Rambault, L. 1993. Conception d'une commande floue pour une boucle de regulation. Thèse de doctorat, Université de Poitiers,212 pages, France.

Rehman, H. U., and Xu, L. 2011. Alternative energy vehicles drive system: Control, flux and torque estimation, and efficiency optimization. *IEEE Transactions on Vehicular Technology*, *60*(8), 3625-3634.

RESEARCHDIVE, 2022. Web site. https://www.researchdive.com/blog/induction-motors-main-types-and-different-applications. Date of access: 05.04.2022

Saad, B., and Goléa, A. 2017. Direct field-oriented control using fuzzy logic type-2 for induction motor with broken rotor bars. Advances in Modelling & Analysis C, 72(4), 203-212.

Sarıgül, I. 2021. Asimetrik altı fazlı asenkron motorun uzay vektör pwm ile doğrudan moment kontrolü. Yüksek lisans tezi, Fırat Ünıversitesi, 115 sayfa, ELAZIĞ.

Tallam, R. M., Habetler, T. G., and Harley, R. G. 2002. Transient model for induction machines with stator winding turn faults. *IEEE Transactions on Industry Applications*, *38*(3), 632-637.

Texas Instruments 1997. Web site. https://www.ti.com/lit/an/bpra048/bpra048.pdf. Date of access: 10.02.2022.

Toufouti, R., Meziane, S and Benalla, H. 2006. Direct torque control for induction motor using fuzzy logic. *ACSE Journal*.

Yordanova, S. 2015. Intelligent approaches to real time level control. *International Journal of Intelligent Systems and Applications*, *7*(10), 19.

Yu, J., Zhang, T., and Qian, J. 2011. Modern control methods for induction motor. Electrical motor products: International energy-efficiency standards and testing methods. WOODHEAD PUBLISHING, pp. 147-159, UK.

Zemmit, A., Messalti, S., and Harrag, A. 2018. A new improved DTC of doubly fed induction machine using GA-based PI controller. *Ain Shams Engineering Journal*, *9*(4), 1877-1885.

APPENDICES

APPENDIX 1. Machine's parameters

APPENDIX 2. Parameters of PI and Fuzzy logic regulators

APPENDIX 1. Machine's parameters

P	4 KW
Rs	1.2 ohm
Rr	1.8 ohm
Ls	0.1554 H
Lr	0.1584 H
Lm	0.15 H
J	0.071 Kg.m^-2
F	0.0001 N.m.s.rad^-1
P	2
E	220 V

APPENDIX 2. Parameters of PI and Fuzzy logic regulator

Ki	0.5
Kp	10
G_e	0.1
G_{ce}	0.0001
$G_{\Delta T}$	100

CURRICULUM VITAE

Personal Information

Name and Surname : Wahib HILOUAN MOHAMED

Education

MSc	Çankırı Karatekin University Graduate School of Natural and Applied Sciences Department of Electronic and Electrical Engineering	2019-Present
Undergraduate	Djibouti University Faculty of Technology Department of Electrical Engineering	2014-2018

Work Experience

Year	**Institution**	**Position**
02-2017-03-2017	Electricity of Djibouti Department of Electric	Traineer.
04-2018-07-2018	Electricity of Djibouti Department of Electric	Agent field Ass